

The carboxyl-terminal extension on DNA polymerase γ of *Saccharomyces cerevisiae* is required for mitochondrial DNA maintenance at 37°C.

**© Copyright by Steven S. Theriault
July 2001**

A thesis submitted in partial fulfillment of the requirements for the degree of

Master of Science

**Department of Microbiology
University of Manitoba
Winnipeg, Manitoba**



**National Library
of Canada**

**Acquisitions and
Bibliographic Services**

**395 Wellington Street
Ottawa ON K1A 0N4
Canada**

**Bibliothèque nationale
du Canada**

**Acquisitions et
services bibliographiques**

**395, rue Wellington
Ottawa ON K1A 0N4
Canada**

Your file Votre référence

Our file Notre référence

The author has granted a non-exclusive licence allowing the National Library of Canada to reproduce, loan, distribute or sell copies of this thesis in microform, paper or electronic formats.

The author retains ownership of the copyright in this thesis. Neither the thesis nor substantial extracts from it may be printed or otherwise reproduced without the author's permission.

L'auteur a accordé une licence non exclusive permettant à la Bibliothèque nationale du Canada de reproduire, prêter, distribuer ou vendre des copies de cette thèse sous la forme de microfiche/film, de reproduction sur papier ou sur format électronique.

L'auteur conserve la propriété du droit d'auteur qui protège cette thèse. Ni la thèse ni des extraits substantiels de celle-ci ne doivent être imprimés ou autrement reproduits sans son autorisation.

0-612-62859-0

Canada

THE UNIVERSITY OF MANITOBA
FACULTY OF GRADUATE STUDIES

COPYRIGHT PERMISSION

**THE CARBOXYL-TERMINAL EXTENSION ON DNA POLYMERASE γ OF
SACCHAROMYCES CEREVISIAE IS REQUIRED FOR MITOCHONDRIAL DNA
MAINTENANCE AT 37°C.**

BY

STEVEN S. THERIAULT

**A Thesis/Practicum submitted to the Faculty of Graduate Studies of The University of
Manitoba in partial fulfillment of the requirement of the degree
of
MASTER OF SCIENCE**

STEVEN S. THERIAULT © 2001

Permission has been granted to the Library of the University of Manitoba to lend or sell copies of this thesis/practicum, to the National Library of Canada to microfilm this thesis and to lend or sell copies of the film, and to University Microfilms Inc. to publish an abstract of this thesis/practicum.

This reproduction or copy of this thesis has been made available by authority of the copyright owner solely for the purpose of private study and research, and may only be reproduced and copied as permitted by copyright laws or with express written authorization from the copyright owner.

ABSTRACT

The mitochondrial DNA (mtDNA) polymerase of *Saccharomyces*, Mip1p, contains a unique carboxyl-terminal extension (CTE) that extends about 300 amino acids past the last conserved motif in the polymerase domain. To analyze the function of the CTE, we created mutant cell lines expressing versions of the mtDNA polymerase lacking 351, 297, 216, or 176 C-terminal amino acids of the CTE. These mutant cells grew normally at 30°C on fermentable and non-fermentable carbon-sources.

However, at 37°C, during growth on glucose, cells expressing the truncated version of the polymerase, Mip1p Δ 351, rapidly lost respiratory ability, while Mip1p Δ 297 cells gradually became respiratory-incompetent. This loss occurred concomitantly with the loss of mtDNA, and was most pronounced in *MIP1* Δ 351 cells. *In organello* replication assays indicate that loss of mtDNA was due to lack of replication competence at 37°C. Together, these results indicate that the amino-terminal one-half of the CTE is required for the maintenance of a functional mtDNA polymerase at 37°C.

Acknowledgements

I would like to thank Dr. Court for her valuable insight, constant patience, and willingness to teach. My thesis would have not been possible otherwise. Special thanks to Dr. Worobec and Dr. Huebner for their help during my thesis and for sitting on my committee. Thanks to my parents and Stephanie who made this thesis possible with their encouragement and constant help. This thesis is dedicated to Chewy. May all the walks he missed be returned ten fold.

Table of Contents

Abstract	i
Acknowledgements	ii
List of Figures	iii
List of Tables	v
List of Abbreviations	vi
CHAPTER 1	
1.1. Introduction	1
1.2. Introduction of polymerase nomenclature	2
1.3. New nomenclature classification	3
1.4. Crystallized DNA polymerases	6
1.5. Comparison between family A DNA polymerases	15
1.6. Mutational analysis of <i>MIP1</i>	18
1.7. Sequence comparison of polymerization subunits	20
CHAPTER 2	
Materials and Methods	23
2.1. Growth media	23
2.2. Mutagenesis	23
2.3. Determination of growth characteristics	26
2.4. Mitochondrial DNA straining	27
2.5. Preparation of mitochondria	27
2.6. Measurement of mtDNA polymerase activity in isolated mitochondria	27
2.7. Antibody production for Mip1p	28
2.8. Protein expression and purification	28
2.9. Sodium dodecylsulfate-polyacrylamide gel electrophoresis	29
2.10. Western immunoblotting of mitochondria	30
CHAPTER 3	
C-terminal Mutants: Results and Discussion	
3.1. Introduction	31
3.2. Development of mutant cell lines	31
3.2.1. Generation of MIP1 Δ 176 mutant cell line	31

mutant cell lines	45
3.3. Insertion of selectable marker	46
3.4. Development of Southern blot probes	50
3.5. Southern blot hybridization	53
3.6. Growth characteristics of mutant cell lines	53
3.7. Radioactive assay to determine polymerase activity	59
3.8. Mip1p detection using Mip1p Antibody	73
3.9. Discussion	73

CHAPTER 4

Appendix	
4.1. Autophagic project	80
4.1.1. Introduction	80
4.1.2. Experimental plan	81
4.1.3. Future work	90

List of Figures

Fig. 1.1. Map of conserved exonuclease and polymerase motifs in the family A polymerases.	8
Fig. 1.2. Schematic drawing of <i>E. coli</i> DNA polymerase.	10
Fig. 1.3. Schematic drawing of T7 DNA polymerase.	13
Fig. 1.4. Regions of homology among the family A DNA polymerases.	17
Fig. 3.1. Ethidium bromide stained agarose gel of PCR fragments from the <i>MIP1</i> gene digested out of pBluescript SK ⁻ .	32
Fig. 3.2. Visual representation of mutant sites within the 3' end of the <i>MIP1</i> gene.	35
Fig. 3.3. Ethidium bromide stained 1% agarose gel of pBS50 vector and the pAS1'F3' vector.	38
Fig. 3.4. Ethidium bromide stained 1% agarose gel of <i>Bam</i> HI digested ligations of <i>HIS3</i> marker and pAS1'F3' plasmid.	40
Fig. 3.5. A. Possible orientation of the <i>HIS3</i> marker in plasmid pAS'F3HIS'.	43
B. Ethidium bromide stained 1% agarose gel of <i>Pst</i> I digested pAS1'F3HIS' plasmid.	44
Fig. 3.6. A. Using restriction enzymes <i>Bgl</i> II and <i>Xho</i> I we can confirm the introduction of the <i>Bgl</i> II site gene within the three mutants.	48
B. Ethidium bromide stained 1% agarose gel of restriction digested mutant plasmids to test.	49
Fig. 3.7. Diagram of restriction digest to allow homologues recombination.	51
Fig. 3.8. A. Diagram of <i>HIS3</i> region in YPH 499, with an internal deletion of	

1042 bp. B. Diagram of <i>MIP1</i> gene with inserted <i>HIS3</i> marker gene.	54
C. Southern blot analysis of <i>HpaI</i>-digested genomic DNA	56
Fig. 3.9. Growth characteristic of mutant cell lines and YPH499.	58
Fig. 3.10. Maintenance of respiratory competence during growth at 37°C.	61
Fig. 3.11. Maintenance of respiratory competence during growth at 37°C.	63
Fig. 3.12. Mitochondrial DNA maintenance at 30°C.	65
Fig. 3.13. Mitochondrial DNA maintenance at 37°C.	67
Fig. 3.14. <i>In organello</i> DNA synthesis by mutant and wild-type mitochondria at 30°C	70
Fig. 3.15. <i>In organello</i> DNA synthesis by mutant and wild-type mitochondria at 37°C	72
Fig. 3.16. Coomassie Blue stained SDS-PAGE of HIS₆Mip protein.	77
Fig. 3.17. Western blot of whole bacterial and purified HIS₆Mip protein extracts.	79
Fig. 4.1. Photographs of cells with enlarged vacuoles	85
Fig. 4.2. DAPI stained yeast cell with/without spherical bodies	89
Fig. 4.3. Electron micrograph of YPH499	92

List of Tables

Table 2.1. <i>E. coli</i> strains used	24
Table 2.2. Yeast strains used	24
Table 2.3. Plasmid and phage used	25
Table 3.1. Restriction sites used for incorporation of Mip1 fragments	34

List of Abbreviations

Å	angstrom
amp^r	ampicillin Resistant
bp	base pair
CTE	carboxyl terminal extension
C-terminus	carboxyl Terminus
DAPI	4,6 diamidino-2-phenylindole
Da	Dalton
DNA	deoxyribonucleic Acid
EDTA	ethylenediamine-Tetraacetic Acid
His₆	hexa-histidiny Tag
IPTG	isopropylthio-β-D-Galactosidase
kb	kilobase
kDa	kiloDalton
LB	Luria-Bertani
μCi	microcurie
μg	microgram
mg	milligram
μl	microliter
ml	milliliter
mM	millimolar
Ni-NTA	nickel-nitriloactetic acid-agarose
³²P	phosphorus 32
PCR	polymerase chain reaction
SDS-Page	sodium dodecylsulfate-polyacrylamide gel electrophoresis
ssDNA	single stranded DNA

CHAPTER 1

1.1. Introduction

Nucleic acid polymerases are enzymes found in all living cells. DNA polymerases are used for the replication and repair of DNA, while RNA polymerases are used for the transcription of DNA into RNA, and reverse-transcriptase is a unique polymerase that can transcribe RNA into DNA. As a group, polymerases perform template directed replication, transcription and repair. They require a single strand of DNA as a template to synthesize a second strand of nucleic acid that is complementary in sequence to the template strand. Within all free-living organisms, the ability to transfer genetic material is vital for the organism's ability to survive and produce viable offspring. For this reason, organisms encode several DNA polymerases that fulfill the multiple tasks of repair and replication within the organism. These replication processes include copying of hereditary material and production of readable copies of genetic material to transcribe and translate into functional proteins. Since DNA polymerases are required for life, their maintenance within the body and their function in replicating genetic material has been studied for decades. Although much is known about DNA polymerases, there is still much to uncover.

All known polymerases are classified into four distinct families; my project began with the realization that there are many differences within the amino acid sequences of polymerases within their respective families. To begin the discussion of my project, an understanding of the classification system used to group polymerases

must be looked at. I will then introduce my project topic with some background thinking and literature findings.

1.2. Introduction of polymerase nomenclature

In the mid 1970's DNA polymerases found in eukaryotes were classified on the basis of size and were assigned a Greek letter based on their order of discovery. This was the simplest approach, which separated all eukaryotic DNA polymerases into four distinct groups (Weissbach *et al.*, 1975). The first polymerases that could be studied were those of high molecular weight (>100,000 Da) and were named DNA polymerase α (Sikorski and Hieter, 1989). These polymerases were found to hold major DNA polymerase activity in cytoplasmic extracts of growing eukaryotic cells, along with being very efficient at copying activated double stranded DNA. These polymerases have also been shown to be acidic in nature and free of 5' \rightarrow 3' exonuclease activity (Sikorski and Hieter, 1989).

The next DNA polymerase to be assigned was DNA polymerase β ; this polymerase is of a low molecular weight (<150,000 Da) and is almost exclusively found in nuclear extracts (Pavco and Van Tuyle, 1985). These enzymes are basic proteins that copy activated DNA very well with little detectable nuclease activity (Weissbach *et al.*, 1975).

DNA polymerase γ is the most recently defined polymerase, it demonstrates the ability to copy A_n-dT_{15} with very high efficiency, but does not copy DNA very well (Yoneda and Bollum, 1965). These polymerases are acidic molecules with a molecular weight of greater than 100,000 Da; they have also been shown to require sulfhydryl-containing compounds for maximal activity (Sikorski and Hieter, 1989).

The last type of polymerase described in the literature, although there will certainly be more, is mitochondrial DNA polymerase (DNA polymerase-mt). As the name implies, this is a sub-cellular mitochondria localized enzyme found in eukaryotes.

As seen above, this type of nomenclature for DNA polymerases has many advantages, the most important being that new polymerases can easily be added to the expandable naming system (Weissbach *et al.*, 1975). A few years after the advent of the Greek letter naming system, mtDNA polymerase assays became more refined. These new assay methods allowed for more accurate quantitation of mtDNA polymerases, and as a result an initial finding using the new assay methods, was the wide spread detection of Mycoplasma within the first HeLa cells used to isolate mtDNA polymerase. The detection of Mycoplasma contamination led to mass controversy over experimental polymerase results when infected HeLa cells were used (Bolden *et al.*, 1976). The controversy was due to the isolation and purification of Mycoplasma polymerase, which was thought to be mtDNA polymerase. As a result, it was found that after the Mycoplasma contamination was removed, mtDNA polymerase had a molecular weight of about 150,000 and could be stimulated by 0.05 to 0.10 M salt. These results, along with the removal of the Mycoplasma contamination and the discovery that mtDNA polymerases also require sulfhydryl containing compounds for activity, allowed for the proper placement of mtDNA polymerase within DNA polymerase family γ (Bolden *et al.*, 1976).

1.3. New nomenclature classification

As sequencing and molecular cloning techniques advanced and the number of identified polymerases increased, the classification system that divided DNA polymerases on the basis of size was becoming outdated and could no longer be used. A new method that was instituted compared the amino acid sequences of all polymerases for conserved regions that could be linked to catalytic function. These catalytic regions include the exonuclease and polymerase regions, which are normally conserved through evolution in related species. With more than 40 different DNA polymerases being grouped based on segments of amino acid sequence similarities, the simple Greek letter nomenclature changed to a more encompassing family classification system (Braithwaite and Ito, 1993). DNA polymerases were reclassified into three major families with a fourth group being introduced, due to its uniqueness from the other families and homology to terminal transferase (Yoneda and Bollum, 1965). The four major groups are comprised of: 1) *Escherichia coli* DNA polymerase I-types (family A), based on conserved regions located at 789-814, 877-998, 1047-1090, 1104-1123, 1131-1158, 1175-1206, 1236-1251, 1284-1305, 1322-1340 and 1365-1376 amino acids, 2) Eukaryotic DNA polymerase α -types (family B), based on conserved regions located at 1407-1760, 1885-1901, 1956-1990, 2081-2100, 2181-2210, 2280-2320, 3) *E. coli* DNA polymerase III α subunits (family C) (due to the large amount of amino acid homology (Braithwaite and Ito, 1993) the specific sequence base pairing will not be listed), and 4) Mitochondrial DNA polymerases. The latter is an undefined group that is still being discussed as to its classification; for this reason I will discuss them in their original placement among family A

polymerases. It has been demonstrated that all family A DNA polymerases are sensitive to dideoxynucleotide inhibitors and are resistant to aphidicolins, which is a defining characteristic that differentiates them from the other families of polymerases. Family A polymerases host a cleanup function during replication, recombination and repair and most carry 5'→3' and 3'→5' exonuclease activity. The 5'→3' exonuclease activity allows for the removal of RNA/DNA primers within the replisome, which is one of the key functions of these polymerases.

Family B DNA polymerases are quite extensive in number and variety, encompassing viral, bacterial and archaeobacterial polymerases; they are sensitive to aphidicolin and resistant to dideoxynucleotide inhibitors. Most contain a highly conserved amino acid sequence motif YGDTD that is suggested to form part of the dNTP-binding site (Ito and Braithwaite, 1990). Since family B polymerases are so extensive, the old nomenclature, using the Greek lettering system based on size and localization within cellular extracts has been modified for the naming of the extensive family B polymerases.

Family C DNA polymerases are differentiated from the other three groups by their homology to *E. coli* DNA pol III α subunit. The family C DNA polymerases are considered the primary replication enzymes within cells, and they are usually multimeric enzymes with at least 10 subunits making up the active polymerase (Ito and Braithwaite, 1990; Braithwaite and Ito, 1993).

Since family A DNA polymerases are the major polymerases being studied in my project, I will describe them in more detail than the other polymerase families.

Family A DNA polymerases, which are all prokaryotic except for fungal mitochondrial DNA polymerases, are classified as being sensitive to dideoxynucleotide inhibitors and resistant to aphidicolin. All family A DNA polymerases share three conserved exonuclease domains and three conserved polymerase domains Figure 1.1 (Ito and Braithwaite, 1990; Braithwaite and Ito, 1993).

A comparison of the active regions for these family A DNA polymerases can be made using other family A DNA polymerases that have been crystallized; active regions defined from the crystal structures can also be used to characterize catalytically important regions within the polymerase family. Using *E. coli* DNA polymerase I as a structural model, we have a tool for the comparison and possible elucidation of the mechanisms used by the enzyme to enhance the fidelity of template-directed polymerization and the origins of polymerase activity.

1.4. Crystallized DNA polymerases

E. coli DNA polymerase I (large fragment) was the first polymerase to be crystallized; it was resolved to 3.3Å while complexed with deoxythymidine monophosphate (Ollis *et al.*, 1985). The crystallized structure shows two distinct regions: the first consisting of ~200 amino acids (324~517 in the polymerase conserved region). This region forms the central, mostly parallel β -pleated sheet, with α -helices on both sides, which is proposed to facilitate deoxynucleoside monophosphate binding (Ollis *et al.*, 1985). There is also a metal binding site formed within this first region, which is located by the carboxylate groups on Asp 355, Glu

Figure 1.1. Map of conserved exonuclease (E1, E2, E3) and polymerase (P1, P2, P3) motifs in the family A polymerases (Ito and Braithwaite, 1991) from *Saccharomyces cerevisiae*, *Neurospora crassa*, *Pychia pastoris*, *Schizosaccharomyces pombe*, T7 phage, *Homo sapiens*, and *Drosophila melanogaster*. This alignment demonstrates that there is a long C-terminal extension in *Neurospora* and *Saccharomyces* polymerases.

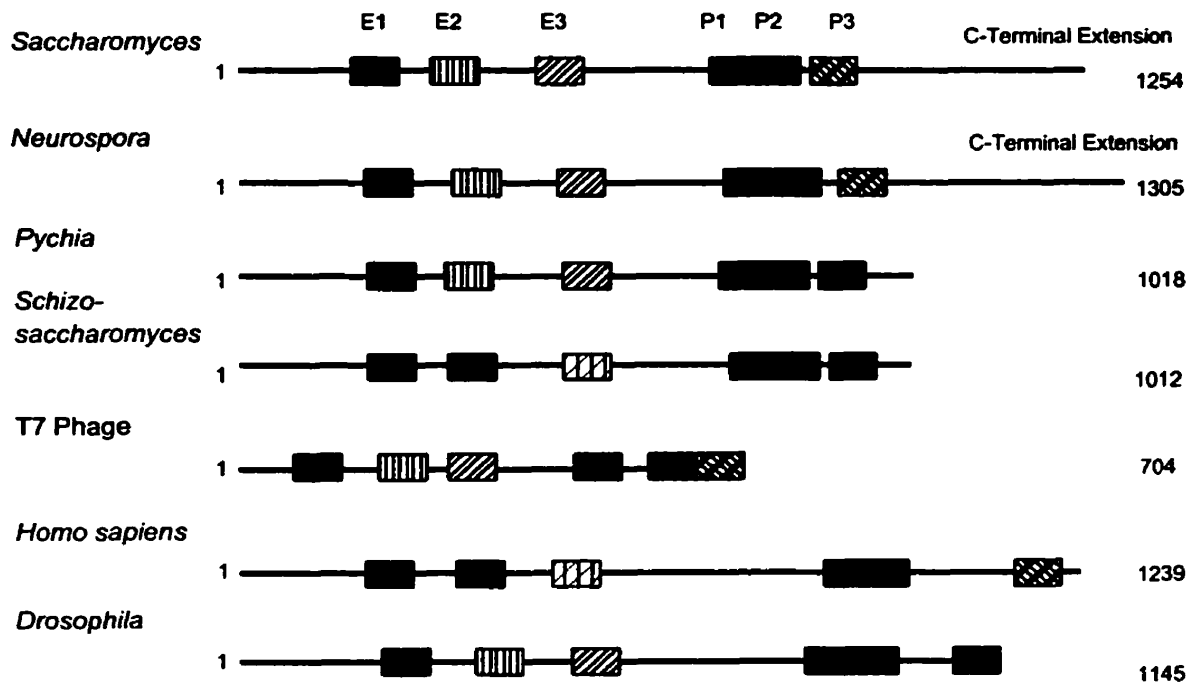


Figure 1.2. Schematic drawing of klenow fragment developed by (Ollis *et al.*, 1985). This drawing demonstrates the classical hand and thumb structure found in most polymerases. The deep cleft is found between helix H and I with the thumb and palm being found around the O helix and R helix respectively. “Regions in β -sheet structure are represented by arrows numbered from the fragment N-terminus and those in α -helix are represented by tubes lettered from the N-terminus” (Ollis *et al.*, 1985).

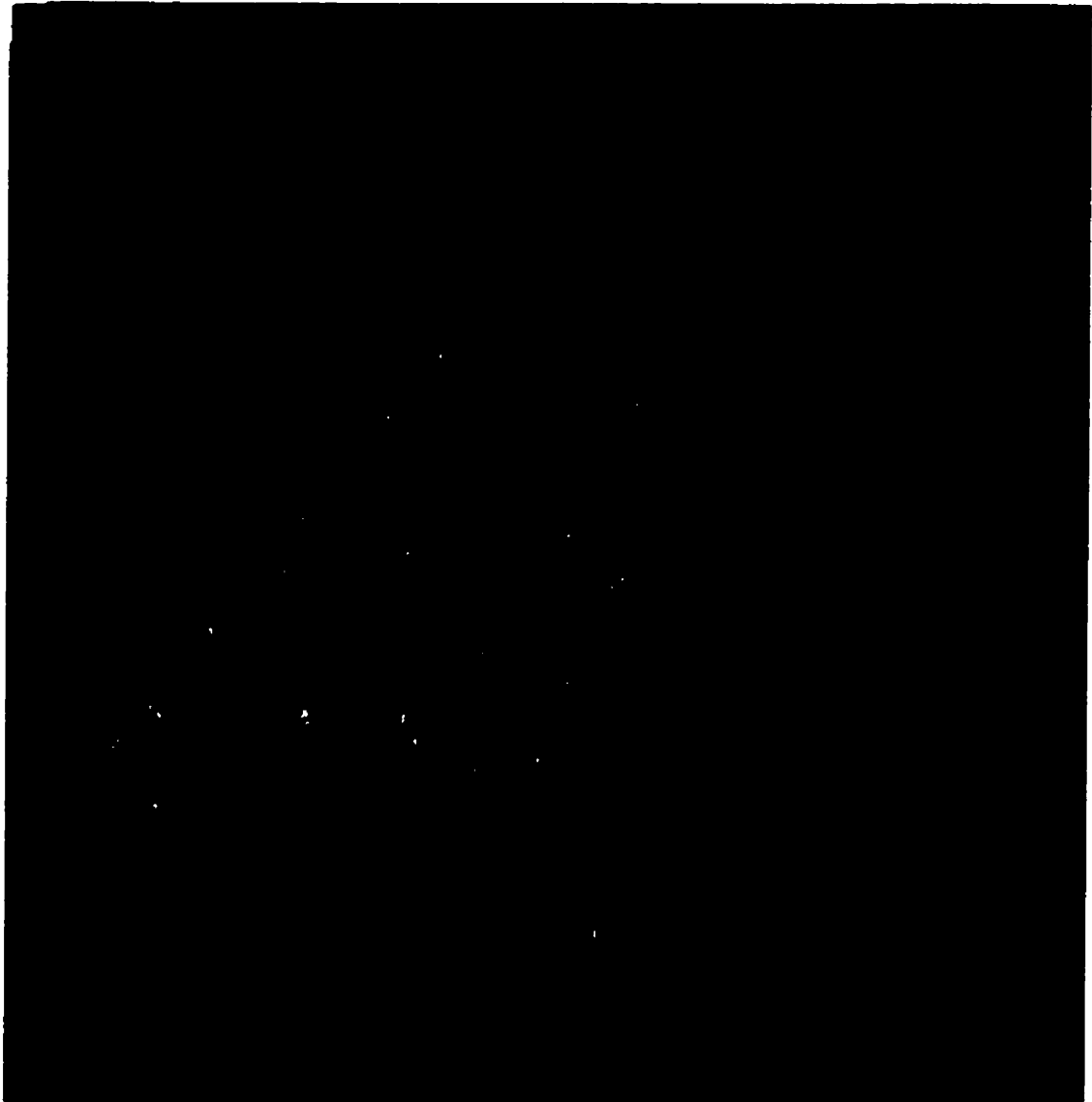
357, Asp 501; the metal binding site also interacts with the 5' phosphate of dTMP, which provides the fourth ligand to the metal binding site.

The second domain is a larger region consisting of 400 amino acids that are in an α -helical conformation, which forms a structure containing a very deep cleft; this structure is the shape of a right hand holding a rod [(Ollis *et al.*, 1985) Figure 1.2]. This structure has a 6-stranded anti-parallel β -sheet that forms the bottom of the cleft, with two large α -helical protrusions forming the sides. The imposing cleft is 20-24Å wide and 25-35Å deep with α -helices J and K protruding into the cleft. The cleft resembles the fingers of the right hand curling in where the cleft opens up on one side of the structure; the opening is around 50Å rather than 20Å. The other wall is formed primarily by two long α -helices, I and H, which form projections of the protein that create a thumb-like overhang (Ollis *et al.*, 1985). These structures form the classical hand diagram used to describe many polymerases.

The large cleft, which fits B-DNA, is suggested to hold the DNA binding site, and the structure of the polymerase suggests a mechanism for its processivity. "The location of a flexibly attached 50 amino acid residue at the tip of the I and H helices suggests that this small sub domain closes off the cleft after DNA binds". This could indicate that the DNA product may be slow to dissociate, which would be indicative of a very processive polymerase (Ollis *et al.*, 1985).

Looking at another polymerases within the family A polymerases, the T7 bacteriophage DNA polymerase has been crystallized at a 2.2Å resolution. In comparing these two crystallized structures (Klenow, T7), we can get a good estimation of the homology between conserved catalytic domains within family A

Figure 1.3. Schematic drawing of T7 DNA polymerase. Helices are represented by cylinders and β -strands by arrows (Doublet *et al.*, 1998). This illustration shows how template DNA (yellow) travels through polymerase and the location of the primer (red).



polymerases. Looking at Figure 1.3, T7 DNA polymerase carries the characteristic right hand shape “in which, the palm, fingers and thumb form the DNA binding groove that leads to the polymerase active site” (Doublie *et al.*, 1998). The palm forms the base of the polymerase active site, presenting three strictly conserved and functionally important acidic regions (Braithwaite and Ito, 1993; Doublie *et al.*, 1998). The T7 DNA polymerase also has the same characteristic folding of the fingers to complete the DNA binding site and bind nucleotides to increase processivity. These similar crystal structures should allow us to compare other family A DNA polymerases with fairly good results.

Comparing yeast species with other eukaryotic species we find some differences within the organization of the mtDNA polymerase. The most striking difference is that in yeast species the mtDNA polymerase is a single subunit, whereas in other eukaryotic species namely *H. sapiens*, *D. melanogaster*, and *X. laevis* the mtDNA polymerase is a multi-subunit enzyme. Within this multi-subunit enzyme two proteins are relevant to my project, the α subunit, which is the catalytic subunit and the β subunit, which is an accessory subunit which is needed for increased processivity of the catalytic subunit (Carrodeguas *et al.*, 1999).

Using sequence homology of conserved motifs and protein secondary structure prediction a comparison was made using *S. cerevisiae*, *N. crassa* and *E. coli* (large fragment species of the family A DNA polymerases) and the α subunits of *H. sapiens*, *D. melanogaster*, and *X. laevis*, mtDNA polymerases, which demonstrated that there is approximately 23% amino acid homology between the two groups. Also the α subunit carries the three conserved polymerase motifs and the three conserved

exonuclease motifs found in all family A DNA polymerases (Lecrenier *et al.*, 1997). It has also been shown that the accessory subunit of animal polymerase γ carries a primer recognition site and/or a processivity clamp which co-purifies with polymerase γ (Braithwaite and Ito, 1993).

1.5. Comparison between family A DNA polymerases

One interesting aspect seen in family A DNA polymerases is the differences in carboxyl-termini. *Saccharomyces* and *Neurospora* mitochondrial DNA polymerases have extended C-termini, while the rest of the family A polymerases, which include *E. coli* DNA polymerase I, and *Streptococcus pneumoniae* DNA polymerase I to name a few, do not. As depicted in Figure 1.4, the mtDNA polymerases in *Saccharomyces cerevisiae* and *Neurospora crassa* have a unique C-terminal extension consisting of around 300 amino acids. This extension is only seen within the mtDNA polymerase of these two organisms; as more genomes are sequenced, other fungal examples may be expected. The extra 300 amino acids in the fungal sequences represent the major difference seen within this family and the function of the 300 amino acids has yet to be discovered.

This novel extension found in mtDNA polymerase of *S. cerevisiae* is not new; Dr. F. Foury first identified it in the late 1980's. Experimental analysis of the mitochondrial DNA polymerase in *S. cerevisiae* began with the development of thermosensitive mutants that were induced by gamma-radiation (Foury and Vanderstraeten, 1992). These mutants gave the first look at the mtDNA polymerase within *S. cerevisiae*, which was found to be responsible for exonuclease activity because some mutant strains lacked this ability. As well, induction of rho⁻ yeast cells

Figure 1.4. Regions of homology among the family A DNA polymerases: yeast mitochondrial DNA polymerases (Mip1), *E. coli* DNA pol I, *E. coli* (E.c.) DNA Q, *Streptococcus pneumoniae* pol I (S.p.), bacteriophage T5, T7, Spo2, and *Thermus aquaticus* (Taq) pol I (Ito and Braithwaite, 1990). Highly conserved regions are indicated by (*), (Ito and Braithwaite, 1990) carried out the sequence alignment.

3' → 5' exonuclease domain

Mip1	167	LVVFDVETLYN ... 220	QVVIGHNVAYDRARVLEEYN ... 337	FQKLANYCATDVTATSQVFD
E.c. pol I	351	VFAFDTEETDSL ... 414	ALKVGQNLKYDRGILANYGI ... 491	LEEAGRYAAEDADVTLQLHL
E.c. DNA Q	8	QIVLDTETTGM ... 93	AELVIHHAAFDIGFMDYEFS ... 146	DALCARYEIDNSKRTLHGAL
S.p. pol I	266	YSGPDVENLKG ... 322	FELFGENYHTDNLVGFSAWSC ... 414	SLYGQTYLVDDDET FYGKGVK
T5	134	PVAFDSETSAL ... 188	HTIVFHNLKEDMHFYKYHLG ... 280	FDIMWPYAAKDTDATIRLHN
T7	1	MIVSDIEANAL ... 55	LIVFHNGHKYDVPALTKLAK ... 164	NEEMMDYNVQDVVVTKALLE
Spo2	3	TLSDIETFSS ... 68	VIKTAYNANFERTCIAKHFN ... 160	WEKFKVYCIQDVEVERAIKN
Consensus		* *	* **	* *

DNA polymerase domain

Mip1	688	CFVGADVSEELWIAS ... 744	SRNEAKIFNYGRIYGAGA ... 884	ARLCISIHDEIRFLVSE
E.c. polI	700	VIVSADYSQIELRIMA ... 753	QRRSAKAINFGLIYGMSA ... 874	VRMIMQVHDELVEVHK
S.p. polI	648	VLLSSDYSQIELRVLA ... 702	DRRNAKAVNFGVVYGISD ... 823	TKMLLQVHDEIVLEVPK
Taq polI	605	LLVALDYSQIELRVLA ... 658	MRRAAKTINFGVLYGMSA ... 777	ARMLLQVHDELVLEAPK
T5	496	RVIAWDLTAEVYYAA ... 561	LRQAAKAITFGILYGS GP ... 700	MKIVMLVHDSVVAIVRE
T7	470	VQAGIDASGLELRCLA ... 517	TRDNAKTFIYGFLYGAGD ... 646	FAYMAWVHDEIQVGCRT
Spo2	381	EFYVSDFAIEARVIA ... 436	LRQKGVAEALALGYQGGK ... 595	YKTMHVHDEAVLDVPR
Consensus		* * • *	• ** ** *	• ** *****

at increased temperatures in mutant phenotypes was observed (Foury, 1982); rho⁻ cells are defined by their inability to respire, which can be induced by the lack of polymerase and/or exonuclease activity. The related processes of lost exonuclease activity and rho⁻ cell development are defined by the lack of repair or replication activity *in vitro*. These activities were tested by the development of erythromycin resistance (mode of action explained below) in these thermosensitive mutants lacking exonuclease activity (Foury, 1982) and the loss of respiratory ability in yeast cells *in vivo* respectively. The loss of respiratory ability was directly correlated with the loss of mitochondrial DNA or mutation of mitochondrial DNA, which led to the loss of mitochondrial function.

Further analysis of the single nuclear gene, which was identified from the above experiments showed that cells with this mutation were deficient in mitochondrial DNA replication and mtDNA polymerase activity (Genga *et al.*, 1989). Using a yeast genomic library and the mutational data from above, the *MIP1* gene was determined to encode the functional mtDNA polymerase. The *MIP1* gene was mapped to the right arm of chromosome XV, and its open reading frame was determined to be 3762 nucleotides long, encoding a basic protein of 143.5 kDa (Foury, 1989). This protein sequence contained characteristic motifs found in other DNA polymerases, confirming its identity as a polymerase. The above results indicated that the *MIP1* gene is required for mitochondrial DNA maintenance and if lost the mitochondria would no longer function in any replicative capacity (Genga *et al.*, 1989).

1.6. Mutational analysis of *MIP1*

Using *in-vitro* mutagenesis, mutated alleles of the *MIP1* gene were constructed in order to locate the important exonuclease regions. The frequency of generation of erythromycin resistance in these mitochondrial mutants was used to determine the effect on proofreading ability of enzymes with single amino acid mutations in the conserved regions of the exonuclease within Mip1p (Genga *et al.*, 1989). Erythromycin resistance can be used as a detection system for proof reading ability on the basis that, if certain mutations are made within the rRNA of the 50S subunit, erythromycin will no longer be able to bind the large subunit of the ribosome and inhibit translocation. Therefore, an increased level of erythromycin-resistant cells indicate a lack in the repair ability of the mitochondrial DNA polymerase.

As expected, cells carrying mutations that mapped to the 3'→5' exonuclease domain showed a 100-400 fold increase in the development of erythromycin resistant mutants. Cells harbouring point mutations made in the polymerase domain and the C-terminal region of *MIP1* only produced 15-50 times more resistant mutants than wild-type (Genga *et al.*, 1989). Mutant cell lines with amino acid substitutions located at T716I, E724K, and P851L in the polymerase domain showed an increase in rho⁻ cell production (>99%) at 37°C. The only mutation produced (R1001I), in the beginning of the C-terminal region showed ~ 25% rho⁻ cell types at both 28°C and 37°C (Genga *et al.*, 1989).

The mutational analysis allowed for a tentative placement of regions within the Mip1p, which are catalytically important. The next logical step was to compare some of the family A DNA polymerases from related species to determine if these

enzymes carry similarity to those in Mip1p of *S. cerevisiae*. Since mitochondrial DNA polymerases are considered to be descendants of bacterial enzymes and are found in all eukaryotic species, their amino acid sequences should be conserved in catalytic regions from yeast to man (Lecrenier *et al.*, 1997). As depicted in Figure 1.1, a multiple amino acid sequence alignment demonstrates that the polymerase γ from *Saccharomyces*, *Neurospora*, *Pychia*, *Schizosaccharomyces*, and the polymerization subunits of *D. melanogaster*, and *H. sapiens* share conserved exonuclease and polymerase regions but differ in their C-termini. Nevertheless, mtDNA polymerases from many species studied to date share many biochemical features. These include the size of their catalytic subunits (100 kDa – 150 kDa), the capacity to copy homoribopolymers, a 3'→5' exonuclease activity, an extreme sensitivity to ethylmaleimide and dideoxynucleotides and resistance to aphidicolin (Foury, 1982; Braithwaite and Ito, 1993). Fungal species, namely *S. cerevisiae* and *N. crassa*, contain the only polymerase within the grouping of family A DNA polymerases to carry an extra 300 amino acids. The exonuclease and polymerase mutational analysis indicate that the extra 300 amino acids in the C-terminal tail of these fungal enzymes are not part of the polymerase or exonuclease catalytic sites. The C-terminal extension may not be a necessary structure for mtDNA polymerase to polymerize DNA and proofread within these fungal species, but it may be used in another manner to help the polymerases function optimally under certain conditions.

1.7. Sequence comparison of polymerization subunits

Amino acid sequence comparison of the polymerization subunit of *H. sapiens*, *X. laevis*, *D. melanogaster* mtDNA polymerases, and the *S. cerevisiae* enzyme

showed that the C-terminal end of the *S. cerevisiae* enzyme does not align with the accessory subunit of higher eukaryotes. This leaves the unanswered question, why is there a three hundred amino acid C-terminal extension in the mtDNA polymerases of lower eukaryotes? If all mitochondria are descended from the same organism, why is there a large difference in the genetic coding of mtDNA polymerases from yeast to man?

One possible explanation comes from the two-subunit structure of other mtDNA polymerases. *Homo sapiens* contain a multiple subunit mitochondrial DNA polymerase, with a larger catalytic subunit and a smaller accessory subunit. The catalytic subunit from a melanoma library when compared to mtDNA polymerase from *S. cerevisiae*, demonstrated 43% homology though the entire polymerase. They both share conserved exonuclease and polymerase domains, which indicates common ancestry (Lecrenier *et al.*, 1997). In addition the accessory subunit from *H.sapiens*, *X. laevis* and *D. melanogaster* has been shown to be related to glycyl-tRNA synthetase from *Thermus thermophilus* (Carrodeguas *et al.*, 1999). The relatively small amount of mtDNA polymerase in cell extracts and the large proportion of nuclear DNA polymerase α , β , δ , ϵ , and ζ has proven to be the limiting factor in the study of mtDNA polymerases. The relative ratios among the polymerases caused isolation problems, which led to difficulties in the characterization of the lower ratio mtDNA polymerase in higher eukaryotes. However, molecular cloning techniques have recently allowed for the purification and study of these mtDNA polymerases (Carrodeguas *et al.*, 1999). Isolation and characterization of mtDNA polymerase from *Homo sapiens*, *Xenopus laevis* and *Drosophila melanogaster* have demonstrated a

common theme among these enzymes from higher eukaryotes; they all require an accessory subunit for efficient processivity of the mtDNA polymerase (Carrodeguas *et al.*, 1999; Johnson *et al.*, 2000; Fan *et al.* 1999). The accessory subunit has been shown to have a brace and clamp like function. As demonstrated by a 3.5-fold tighter binding (k_d of 9.9 +/- 2.1 nM compared to 39 +/- 10 nM) than for the catalytic subunit alone (Johnson *et al.*, 2000). It was also demonstrated that, with the addition of the accessory protein nucleotide binding was increased 6-fold with a DNA polymerization rate increase of 5-fold (Johnson *et al.*, 2000). The above increases were confirmed by an increase in processivity of nearly 10-fold. This accessory subunit has not been found in lower eukaryotes (*S. cerevisiae* and *N. crassa*) (Lecrenier *et al.*, 1997).

These results led us to the imposing question, is there a function of the 300 amino acid C-terminal extension in yeast mtDNA polymerase and is it related to the accessory subunit of animal polymerase γ ? To begin answering questions on the role of the C-terminal end in *S. cerevisiae* a series of mutants lacking parts of the C-terminal end were created. The ability of the mutants to faithfully replicate mtDNA was examined using the methods described herein.

CHAPTER 2

MATERIALS AND METHODS

2.1. Growth media

Yeast strains were grown on the following media: YPG (1% yeast extract, 1% peptone, 3% glycerol); YPAD (1% yeast extract, 1% peptone, 2% dextrose, 0.002% adenine hemisulphate); SC-HIS (6.7% nitrogen base, 4% dextrose, all amino acids except histidine); YPG-erythromycin (3% glycerol, 2% peptone, 0.5% potassium phosphate, 0.15 g/L erythromycin); Luria-Bertani media (LB) and the appropriate antibiotics were used to transform and maintain *E. coli* strains.

2.2. Mutagenesis

Mutant versions of mitochondrial DNA polymerase were generated by site-directed mutagenesis (Kunkel *et al.*, 1987) using the Muta-Gene kit from Bio-Rad (Mississauga Canada). The template DNA was plasmid pMIP1-F3, which contains basepairs (bp) 2615 to 3840 of the coding sequence of Mip1p preprotein and extends 34 bp past the stop codon. Primers were used to introduce a stop codon [**BOLD**] followed by a *Bgl*II site [underlined] for insertion of the selectable marker *HIS3* into the *MIP1* gene. The stop codons were introduced at positions 3192, 2949, and 2787 of the *MIP1* coding sequence to create the genes *Mip1*Δ216, *Mip1*Δ297, and *Mip1*Δ351, respectively.

The primers used for the site-directed mutagenesis were synthesized by Canadian Life Technologies Inc., (Burlington, Canada) and are as follows:

for *Mip1*Δ351: 5'GCGAAAAGGACAAATAGATCTCAGAGCTGCTATGG;

Table 2.1 *E. coli* strains used in this project.

Table 2.1 *E. coli* strains used in this project.

Bacterial Strains	Characteristics	Reference
DH5 α	<i>supE44</i> Δ <i>lacU169</i> (ϕ 80 <i>lac</i> Δ M15) <i>hsdR17 recA1 endA1 gyrA96 thi-1 relA1</i>	(Hanahan, 1983)
CJ236	<i>dut1 ung1 thi-1 relA1</i> pCJ105 (cam ^r F')	(Kunkel <i>et al.</i> , 1987)
M15 rep	<i>nal^r str^r rif^s lac⁻ ara⁻ gal⁻ mtl⁻ recA⁺ uvr⁺</i> pREP4 (lacI kan ^r)	(Villarejo and Zabin, 1974)

Table 2.2 Yeast strains used in this study.

Yeast strains	Characteristics	Source
<i>S. cerevisiae</i> YPH499	<i>MATα</i> , <i>ura3-52</i> , <i>lys2-801^{amber}</i> , <i>ade2-101</i> , <i>trp1</i> Δ 63, <i>his3</i> - Δ 200, <i>leu2</i> Δ I	(Sikorski <i>et al.</i> , 1989)
<i>S. cerevisiae</i> S150	<i>MATα</i> <i>leu2-3,112 his 3</i> - Δ 1 <i>trp-289 ura 3-52</i>	(Steger <i>et al.</i> , 1990)

Table 2.3 Plasmids and phage used in this project.

Plasmid or phage	Characteristics	Source
pBluescript SK ⁻	<i>amp</i> ^r , Blue/white color screening, Bacteriophage T3 and T7 promoters, ssDNA fl (-) origin of replication	Stratagene
PQE-10	<i>amp</i> ^r , <i>E. coli lacP</i> , ribosome binding site, N-terminal His ₆ -tag	Qiagen
pAS1	<i>amp</i> ^r , <i>trp</i> ^r , Gal4 binding domain, 2μ origin of replication.	(Gietz <i>et al.</i> , 1997)
pFL39	pUC19 vector with a <i>Bgl</i> II cassette containing the <i>TRP1</i> gene and a <i>Clal</i> cassette containing CENVI plus ARS	(Foury and Vanderstraeten, 1992)
pBS50	pBluescript SK ⁻ vector with <i>Bam</i> HI cassette with <i>HIS3</i> gene	Steiner*
pMIP1-f3	<i>amp</i> ^r , Blue/white color screening, Bacteriophage T3 and T7 promoters, ssDNA fl (-) origin of replication	Steven**
R408	Helper phage for ssDNA production from pBluescript SK ⁻	Promega

* Plasmid was a gift from H. Steiner University of Munich

** Created by author of thesis

for *Mip1*Δ297: 5'CTGCATAACCCCCTAGATCTCGAACAAAACCGCC
and *Mip1*Δ216: 5'GGCTAGAAGATGAGTAGATCTGCGGGAGTGTAC.

The sequences of the regions to be expressed as part of the mutated polymerases were confirmed by DNA sequencing. The developed *Bgl*III site was used for the insertion of a *Bam*HI fragment of pBS50 containing the *HIS3* gene. The mutated sequences were released from pBluescript SK⁻ by digestion with *Xba*I and transformed into YPH499 using the lithium acetate method (Gietz *et al.*, 1997). Insertion of the proper mutation cassette at the correct position was confirmed by Southern blot analysis of digested DNA using *HIS3* and *MIP1* sequences as probes.

To create the coding sequence for *Mip1*Δ176, the *Bam*HI fragment containing the *HIS3* marker was ligated into the *Bam*HI site in pMIP-F3 at position 3310 bp of the *MIP1* gene. The resulting disruption construct was introduced into YPH499 and its location was confirmed as described above. The *Mip1*Δ176 construct encodes an additional ten C-terminal amino acids (AARSCSLACT) due to the extension of the reading frame into the *HIS3* cassette.

2.3. Determination of growth characteristics.

The respiratory ability of the mutant cell lines was tested by growth on glycerol-containing media (YPG) and dextrose-containing media (YPAD), at normal (30°C) and increased growth temperature (37°C). All cells were taken

from glycerol stocks, grown for approximately 12 hours in YPAD at 30°C, then diluted to 0.10 OD_{600nm} /ml in the appropriate medium and cell growth was monitored by absorbance at OD_{600nm}. Cell growth was observed in both batch culture from 0 to 5 days and in cultures that were diluted to 0.002 OD_{600nm}/ml in fresh media every 24 hours. Serial dilutions of cells were plated on YPG, YPAD, and SC-HIS at 24 hour intervals.

2.4. Mitochondrial DNA staining.

Mitochondrial DNA maintenance during growth was assessed by staining cells with 4', 6-diamidino-2-phenylindole (DAPI). For staining, 1 ml of cells at 1 OD_{600nm}/ml were pelleted by centrifugation, and resuspended in 50 µl of distilled water, 1 ml of 50% ethanol and 0.1-0.2 µg DAPI. Cells were rinsed three times with distilled water and resuspend in 20 µl of distilled water. Visualization was carried out using Zeiss Epi-fluorescent microscopy using a 1000X oil emersion lens.

2.5. Preparation of mitochondria.

Strains were grown in 1 liter of YPAD at 30°C. Cells were harvested at 1 OD_{600nm}; transformation to spheroplasts was accomplished with lyticase (Sigma-Aldrich, 800units/mg). Mitochondria were isolated by differential centrifugation and immediately frozen in liquid nitrogen and stored at -60°C (Daum *et al.*, 1982). Protein concentration was determined using Bradford assay (Sigma-Aldrich) and the mitochondrial content of the extracts was estimated by assaying Malate Dehydrogenase activity (Kitto, 1969).

2.6. Measurement of mtDNA polymerase activity in isolated mitochondria.

Analysis of mtDNA synthesis was carried out as described in (Duchniewicz, Germaniuk, *et al.* 1989, using 1.0 mg/ml [total protein] in 50 μ l of reaction buffer containing 10 μ Ci [α - 32 P] dTTP (NEN, Boston, MA) as radioactive label. The rate of incorporation of radioactive dTTP was measured at 5 min intervals at 30°C and 37°C by precipitation of labeled mtDNA with 750 μ l 10% trichloroacetic acid and 100 mM sodium pyrophosphate. Precipitates were collected on GF/C Whatman glass fiber filters, and washed four times with 2 ml of 1 M hydrochloric acid and 100 mM sodium pyrophosphate and once with 4 ml of ethanol. The filters were dried and transferred to scintillation fluid and counted on a Beckmann LS 6500.

2.7. Antibody production for MIP1p

To prepare for the production of an antibody for *MIP1*, a restriction digest of pFL34 (*MIP1*) using *Bam*H1 and *Hind*III was carried out. A 0.9 kilo-base fragment was purified from a 1% agarose gel by electrophoresis onto a DEAE cellulose membrane (Ropp and Copeland, 1996) and salt extraction was carried out using the manufacturer's protocols. The extracted fragment was ligated into a pQE-10 vector, which was also cut with *Bam*H1 and *Hind*III. T4 DNA Ligase (Life Technologies, Burlington, ON) was used to ligate the two fragments together, resulting in a construct containing pQEMIP1 fragment with the coding sequence for N-terminal hexahistidinyI (His₆). The N-terminal tag of histidines is used in the purification of the translated product after expression in *E. coli*. The proper insertion of the 0.9 kb fragment was determined using restriction digest analysis.

2.8. Protein expression and purification

His₆ Mip1p was purified according to Qiagen protocols and cultures of *E. coli* M15 rep containing pQEMIP1 plasmid were grown overnight in LB broth and then they were diluted 1/10 and grown to A_{600} 0.7-0.9 in fresh LB broth. The induction of protein expression was facilitated using isopropylthio- β -galactoside (IPTG) at a final concentration of 2 mM, followed by growth for an additional 4 hours. Centrifugation at 4000xg was used to harvest cells; lysis of cells was carried out using Buffer B (8 M urea, 0.1 M NaH_2PO_4 , 0.01 M Tris, pH 8.0) and the histidine tagged protein was bound using Ni-NTA agarose resin, which binds the *His₆* tag. Buffer C (8 M urea, 0.1 M NaH_2PO_4 , 0.01 M Tris-HCl, pH 6.3) was used to remove any non-bound protein and multiple wash steps were used to ensure protein purity. The *His₆* tagged protein was eluted using Buffer C/100 mM EDTA, and proteins were run on a sodium dodecylsulfate-polyacrylamide gel (SDS-PAGE) to ensure purity. The protein was sent to Immuno-Precise Antibodies Ltd. for polyclonal antibody production.

2.9. Sodium dodecylsulfate-polyacrylamide gel electrophoresis

SDS-PAGE gels were performed using a 12% separating gel covered by a 7.5% stacking gel and 7% separating covered by a 5% stacking gel, depending on the size of the protein (Sambrook *et al.*, 1989). Loading buffer containing 50 mM Tris-HCl, pH 6.8, 7% (v/v) glycerol, 1.3% (w/v) SDS, 0.01% (w/v) bromophenol blue and 0.5% (v/v) β -mercaptoethanol was used when loading all protein samples. All samples were also heated to 100°C for 10 min prior to electrophoresis and all gels were run with low or high molecular weight markers (Sigma, Oakville, ON, Canada) depending on the size of the protein being examined. Electrophoresis was carried out

at 100-150 V for 1 hour, gels were stained with Coomassie Blue staining solution (0.1% (w/v) Coomassie Brilliant Blue G-250, 40% (v/v) methanol and 10% (v/v) acetic acid) and destained with 40% methanol, 10% acetic acid.

2.10. Western immunoblotting of mutant strains run on SDS-PAGE gels

Whole mitochondrial extracts isolated as described above were run on a SDS-PAGE gel (preparation described above). Mini Trans-Blot Transfer Cell (BioRad) was utilized for the transfer of proteins from the SDS-PAGE gel to a Trans-Blot nitrocellulose transfer membrane (BioRad) according to manufacturer's specifications. Samples were transferred at 4°C with a constant current of 400 mA for 1 hour in transfer buffer containing 25 mM Tris-HCl, pH 8.3, 192 mM glycine and 20% (v/v) methanol. The nitrocellulose membrane was immunostained using standard immunoblotting protocols (Thompson *et al.*, 1994). The membrane was incubated to block non-specific binding of the Mip1 antibody using TBS buffer (10 mM Tris-HCl, pH 7.5, 150 mM NaCl) containing 5% non-fat milk for 30 min. A 1:1000 dilution of anti-Mip antiserum (described above) was added to the membrane and incubated for an additional hour; a second antibody, goat-anti-rabbit IgG conjugated to horseradish peroxidase (Sigma, Oakville, ON, Canada) was diluted to 1:2000 in TBS in non-fat milk and added to the membrane for 1 hour. In between each successive step the membrane was washed with TBS + Tween 20 to remove any non-specifically bound antibody and with TBS to remove the excess Tween 20. After incubation and washes were complete the blot was treated with ECL Luminol reagents 1 and 2 (Amersham Life Science Inc., Oakville, ON, Canada) and exposed to Kodak (X-OMAT) film for 1-5 min for protein band detection.

CHAPTER 3

RESULTS AND DISCUSSION

3.1. Introduction

The study of the C-terminal end of *S. cerevisiae* began with the isolation of a fragment of yeast DNA containing the C-terminal coding sequence. Using this isolate we developed mutant C-terminal cell lines using site-directed mutagenesis. Utilizing polymerase chain reaction, the *MIP1* gene was amplified into three fragments; these amplicons were created from the vector pFL39 *MIP1* which was kindly provided by Dr. Foury's lab; the resulting fragments were named F1, F2, and F3, which correspond to base pairs 457-1715, 859-2811, and 2120-3883 in the *MIP1* gene respectively. The resulting PCR products (Figure 3.1) from the above reactions were blunt-end ligated into a pAS1 vector and a pBluescript SK⁻ vector (see Table 3.1 for enzyme sites) to allow for simpler manipulation of the DNA (M. Li constructed the above plasmids). pAS1 was used as a vector with the capability of being maintained as a plasmid in both yeast strains and bacterial strains; pBluescript SK⁻ was used as a mutagenic vector for ssDNA production in *E. coli*.

3.2. Development of mutant C-terminal cell lines

The strategy for the development of the C-terminal mutants was to create a stop codon to disrupt the translation of the Mip1p protein at four different regions (Figure 3.2) and to insert a marker gene to allow identification of mutant cells.

3.2.1. Generation of MIP1 Δ 176 mutant cell line

Using the pAS1'F3' vector, the F3 sequence was restriction digested using *Bam*HI, which cuts at bp 3310. This created a single cut within the vector, which

Figure 3.1 Ethidium bromide stained agarose gel of PCR fragments from the *MIP1* gene digested out of pBluescript SK⁻. Lane 1, 1 Kb⁺ ladder (Gibco-BRL); Lane 2, pBluescript SK⁻‘F1’ digested with *SalI* and *XbaI*; bands represent the 1.2 kb F1 fragment and a 3.0 kb fragment of pBluescript; Lane 3, pBluescript SK⁻‘F2’ digested with *SalI*; bands represent 1.9 kb fragment F2 and a 3.0 kb fragment of pBluescript; Lane 3, pBluescript SK⁻‘F3’ digested with *SalI* and *XbaI* bands represent 1.7 Kb fragment of F3 and a 3.0 kb fragment of pBluescript.

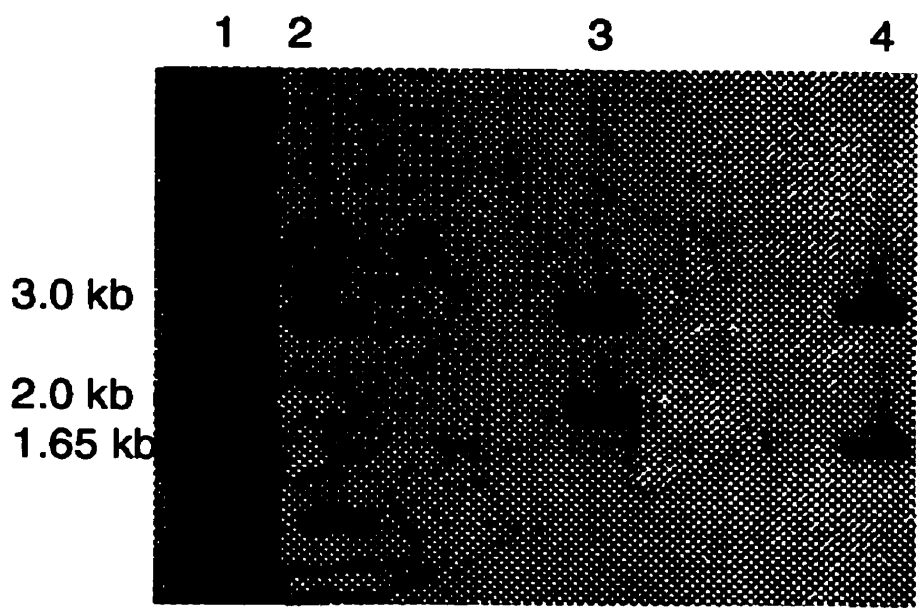
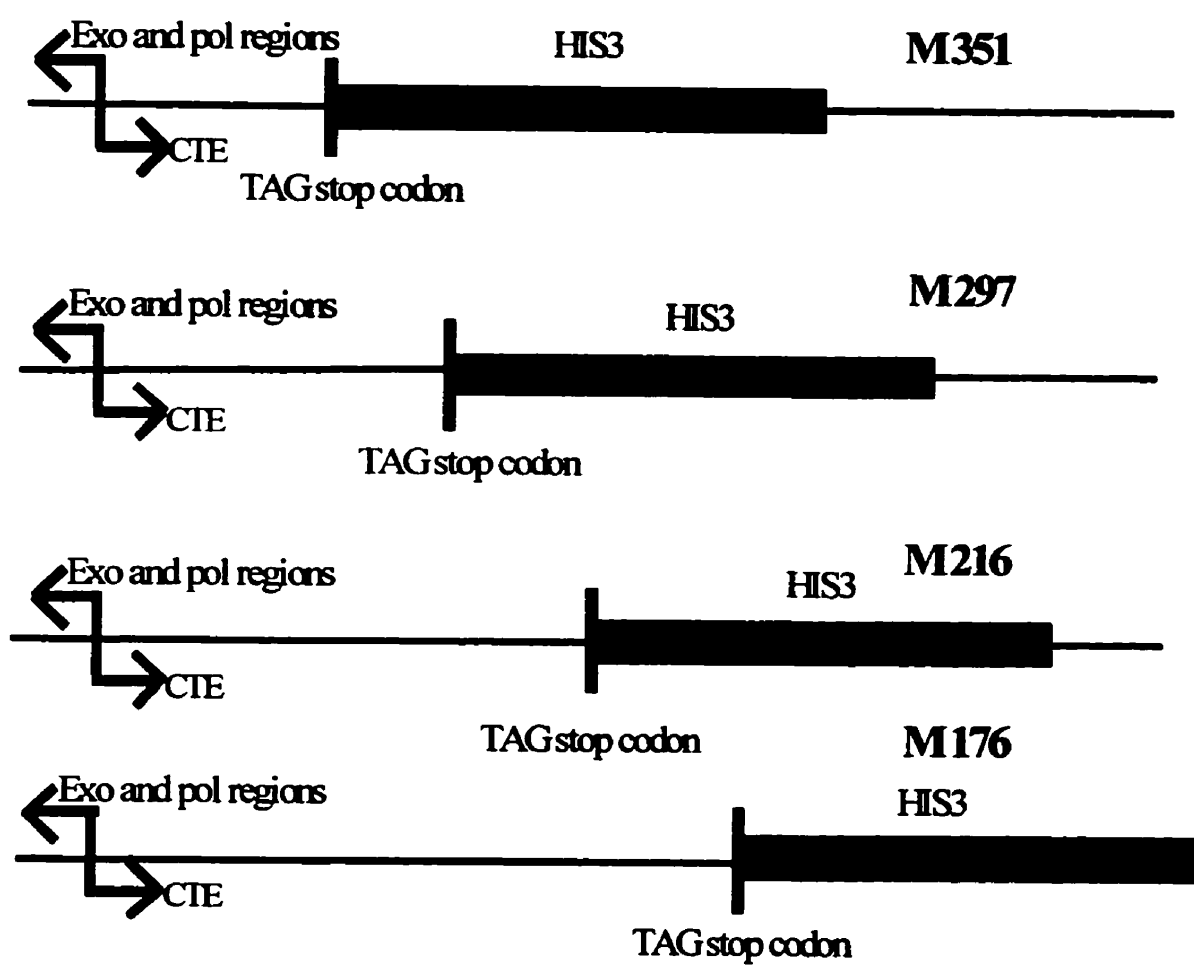


Table 1 Restriction sites used to incorporate fragments of Mip1 into pAS1 and pBluescript SK⁻

Plasmid fragment name	5' restriction enzyme	3' restriction enzyme	Vector
F1	<i>NcoI</i>	<i>SalI</i>	pAS1
F2	<i>NdeI</i>	<i>SalI</i>	pAS1
F3	<i>NcoI</i>	<i>SalI</i>	pAS1
F1	<i>SalI</i>	<i>SalI</i>	pBluescript SK-
F2	<i>SalI</i>	<i>NdeI</i>	pBluescript SK-
F3	<i>EcoRI</i>	<i>EcoRI</i>	pBluescript SK-

Figure 3.2. Visual representation of mutant sites within the 3' end of the *MIP1* gene. The *HIS3* marker is represented by the full bar, stop codons and *Bgl*II sites are demonstrated by a vertical line and arrows indicate the relative position of the polymerase (pol) and exonuclease (exo) coding sequences in reference to their location within *MIP1*.



corresponds to a single DNA fragment 7.1 kb in size (Figure 3.3). pBS50 was used as a source for the *HIS3* marker gene, which was digested out of the vector using *Bam*HI. The two fragments that were produced consisted of a fragment of 3.8 kb and a fragment of 1.7 kb, corresponding to the pBS50 vector and the *HIS3* marker gene, respectively (Figure 3.3). Dephosphorylation of the *Bam*HI cleaved pAS1 F3 plasmid was carried out using calf alkaline phosphatase (Gibco-BRL) according to manufacturer's instructions and the 1.7 kb *HIS3* fragment was purified using DEAE-cellulose gel extraction protocol (Sambrook *et al.*, 1989). The dephosphorylated vector and the purified marker DNA were ligated together using T4 DNA ligase in the appropriate buffer. The ligation mixture was transformed into DH5 α competent *E. coli* cells (Sambrook *et al.*, 1989) and grown for individual colony selection on LB+ ampicillin agar. The resulting colonies were isolated and inoculated into LB+ ampicillin broth for plasmid DNA isolation. Correct ligation products were tested by restriction digest analysis of potential plasmids with *Bam*HI (Figure 3.4); correct ligation reaction would produce a 1.7 kb insert fragment and a 7.1 kb pAS1 fragment. One plasmid, which was isolated pAS1/F3/*HIS3* was chosen for further study. The orientation of the *HIS3* marker within this plasmid was determined using the restriction enzyme *Pst*I, which when used to digest the above plasmid produced a 1.2 kb fragment when the *HIS3* gene is in the 'sense' orientation by digesting within the vector and in the *HIS3* marker (Figure 3.5 A,B) the colony in which the plasmid DNA was isolated from was renamed pAS1/F3/*HIS3*S and used for further experimentation.

Figure 3.3. Ethidium bromide stained 1% agarose gel of pBS50 vector and the pAS1'F3' vector. Lane 1, Lambda ladder (Gibco-BRL); Lane 2, pBS50 vector digested with *Bam*HI restriction enzyme, this removed the *HIS3* marker gene (1.7 kb) from the pBS50 vector (3.0 kb). Lane 3, pAS1'F3' was linearized using the restriction enzyme *Bam*HI.

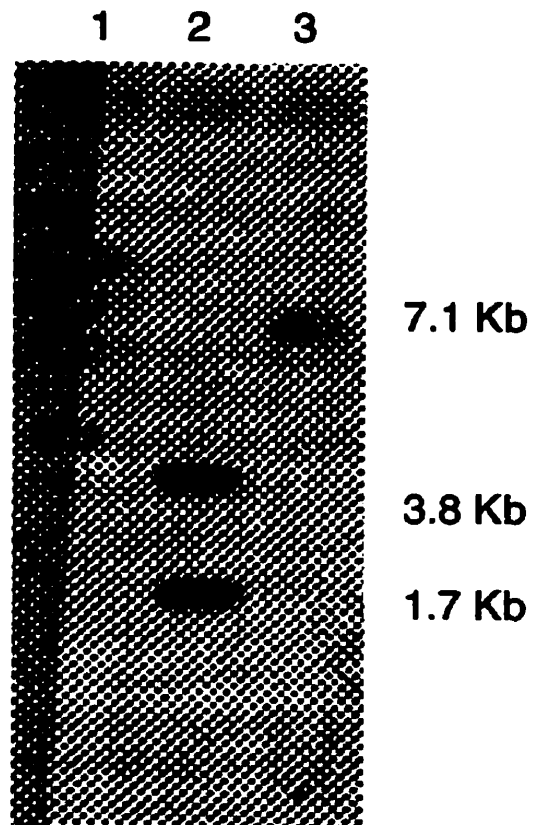


Figure 3.4. Ethidium bromide stained 1% agarose gel of *Bam*HI digested plasmids from ligations of *HIS3* marker and pAS1'F3' plasmid. Lane 1, Lambda ladder (Gibco BRL); Lanes 2,3 and 4, positive clones from the ligation reaction of the *HIS3* marker into the pAS1'F3' vector. The *HIS3* marker is seen at 1.7 kb and the vector is at 7.1 kb.

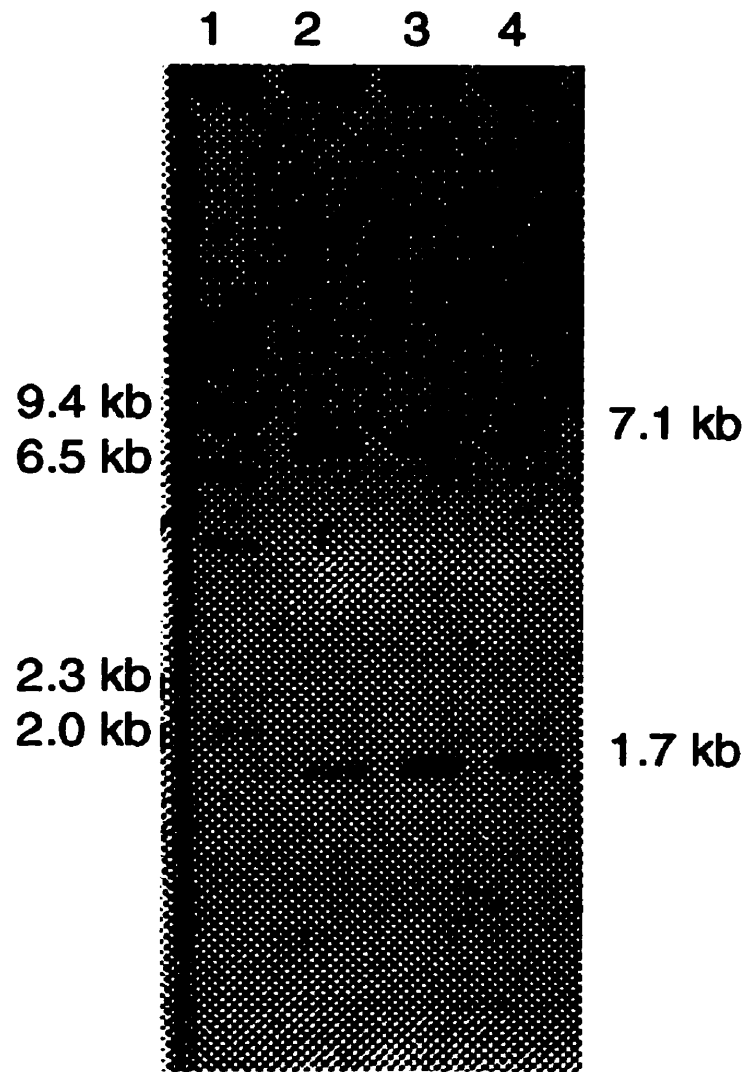
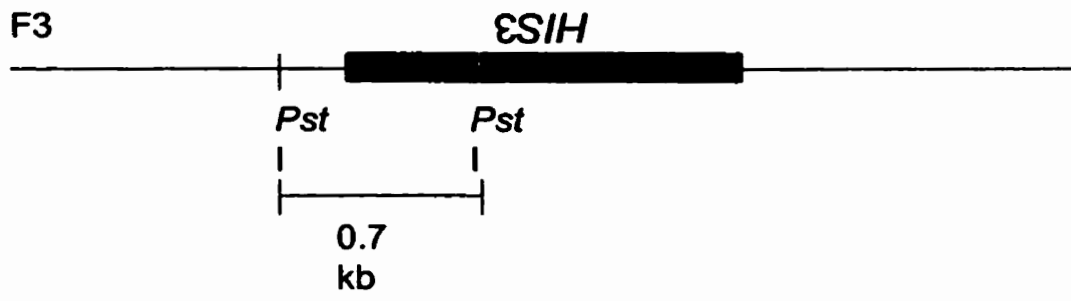
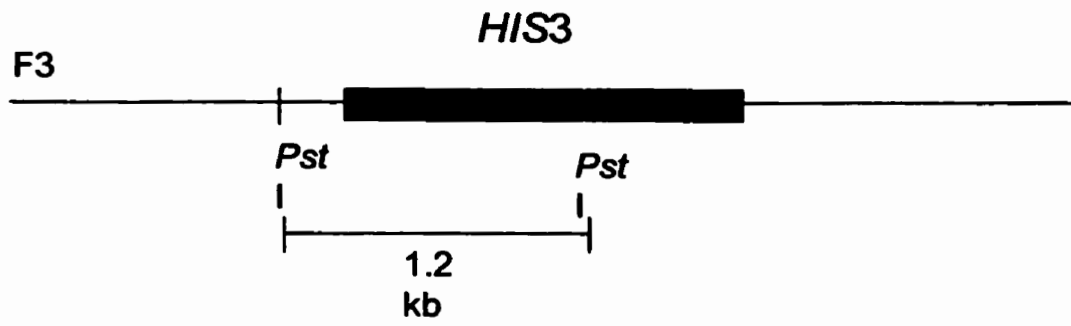
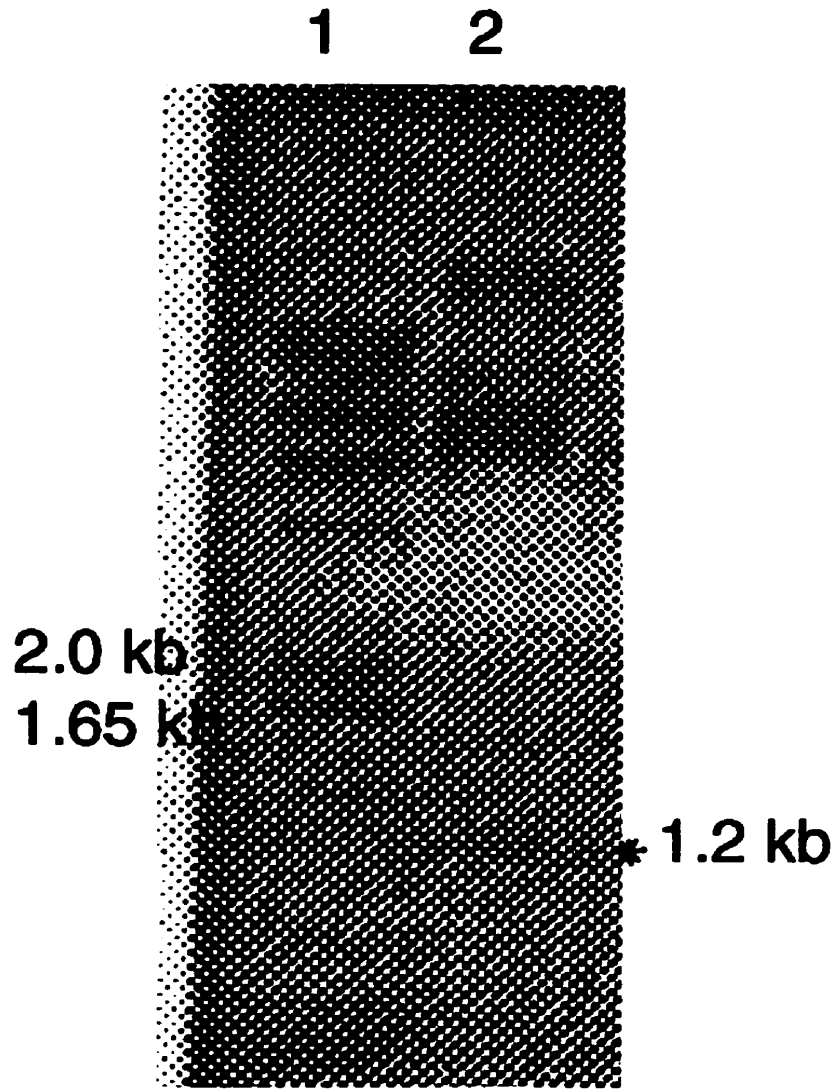


Figure 3.5. A. Possible orientation of the *HIS3* marker in plasmid pAS'F3HIS'. Thin and thick lines indicate F3 DNA and *HIS3* marker, respectively. Sizes of the *Pst*I fragments predicted for each orientation of *HIS3* are given below. B. Ethidium bromide stained 1% agarose gel of *Pst*I digested pAS1'F3HIS' plasmid. The orientation of the *HIS3* marker could be ascertained by this digestion, Lane 1, Lambda ladder (Gibco-BRL); Lane 2, pAS1'F3HIS' digested with *Pst*I the 1.2 kb fragment indicates the *HIS3* marker is in the proper orientation. Astrix indicates position of band 1.2 kb, band was visible in original but did not reproduce in printed form.

A



B



To transfer this mutant coding sequence to a yeast system for functional analysis, the above plasmid was digested with restriction enzymes *SalI* and *NcoI* which released the F3::*HIS3* segment and allowed for the transformation into a yeast strain YPH499 following lithium acetate transformation procedures (Gietz *et al.*, 1997). The transformation mixture was spread on SC-HIS agar plates to select for yeast cell lines with functional histidine pathways, indicating that the transformation and homologous recombination of the mutated F3 fragment with the *HIS3* marker was a success. Isolated colonies were again streaked on SC-HIS agar plates for single colony isolation of possible mutant cell lines. Southern blot analysis was carried out on the isolated mutants (Figure 3.8) and positive mutant cell lines were renamed Mip1Δ176.

3.2.2. Generation of Mip1Δ216, Mip1Δ297, and Mip1Δ351 mutant cell lines

The strategy in developing the other three mutants was to introduce a stop codon followed by a *BglII* site, to allow the insertion of a selectable marker.

Development of the other three mutants was carried out using site-directed mutagenesis. Primers used for mutagenesis are listed in Chapter 2 and were obtained from Gibco-BRL. Mutagenesis was carried out using these primers and ssDNA obtained from the pBluescript vector with the F3 insert according to the protocol in Methods of Enzymology (Kunkel *et al.*, 1987). After synthesis of mutated F3 fragments, the reaction mixtures were transformed in DH5α *E. coli* cells for amplification and plated on LB+ ampicillin agar to isolate colonies. Colonies were picked and grown further in LB+ ampicillin broth, plasmid DNA was isolated from the cell cultures using standard isolation techniques and digested with *BglII* and *XhoI*

restriction enzymes to identify correctly mutagenized fragments (Figure 3.6B). DNA synthesis using the mutagenic primer generated the *Bgl*II restriction site at different positions in each *Mip1*Δ216, *Mip1*Δ297, and *Mip1*Δ351 and the *Xho*I site is present in the vector's multiple cloning site Figure (3.6A).

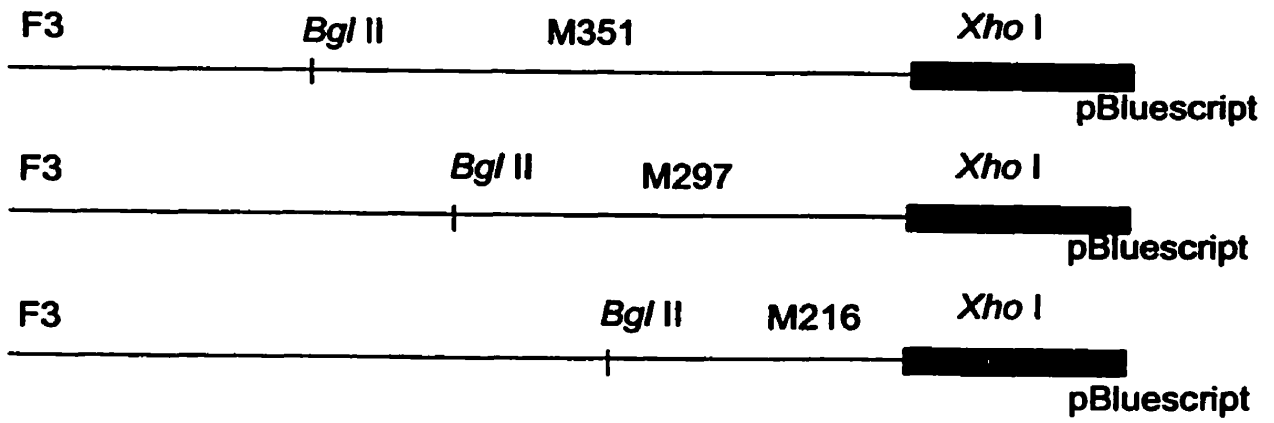
Now a set of mutants encoding mtDNA polymerases lacking 176, 216, 297 or 351 amino acids from the carboxyl-terminus of the *Mip1p* protein had been created. *Mip1p*Δ351 lacks the majority of a highly conserved segment following the third polymerase domain, while *Mip1p*Δ297 terminates within the last four amino acids residues of this conserved region. *Mip1p*Δ216 and *Mip1p*Δ176 encode proteins lacking about half of the C-terminal end.

3.3. Insertion of a selectable marker

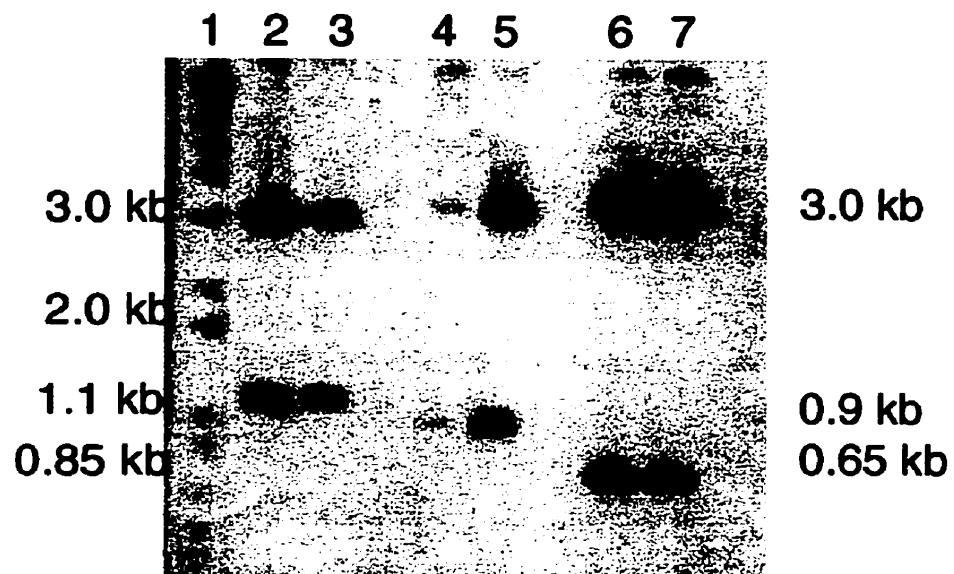
In order to be able to select and identify mutant cell lines with the mutagenized *MIP* genes, a *HIS3* marker was ligated into the *Bgl*II site that was introduced by mutagenesis. The *HIS3* marker was digested out of plasmid pBS50 using the restriction enzyme *Bam*HI and separated on a 1% agarose gel; the resulting 1.7 kb fragment was isolated using DEAE cellulose extraction to prepare the *HIS3* marker for ligation. The three mutated F3 plasmids were digested with *Bgl*II and dephosphorylated using calf-intestinal alkaline phosphatase. Ligation of the *HIS3* marker gene was conducted using T4 DNA ligase; the subsequent plasmids were transformed into DH5α competent cells and positive clones were selected using LB-ampicillin agar. The correct ligation of the plasmid and insert was confirmed using *Xba*I and *Xho*I restriction enzymes (data not shown). The *Xba*I site is located in the pBluescript vector and in the *MIP1* gene at 3824 bp; the *Xho*I site is located within

Figure 3.6. A. Diagram of cleavage site for restriction enzymes *Bgl*III and *Xho*I which were used to confirm the introduction of the *Bgl*III site gene within the three mutants. Thin and thick lines represent F3 fragment and vector respectively. The plasmids are drawn in linear form for simplicity. Note that the vector portion of the DNA is not drawn to scale. B. Ethidium bromide stained 1% agarose gel of restriction digested mutant plasmids to test. Lane 1, 1 Kb⁺ ladder (Gibco-BRL); Lanes 2-7, Mutagenized plasmid DNA digested with *Bgl*III and *Xho*I. Lane 2, 3, pBluescript 'M351' releasing a 1.1 kb fragment; Lane 4, 5, pBluescript 'M297' resulting in a 0.9 kb band; Lane 6, 7, pBluescript 'M216' releasing a 0.65 kb fragment.

A



B



the *HIS3* marker at 1097 bp. Using these two restriction enzymes we can determine correct insertion and orientation of the *HIS3* gene. Mutants before *HIS3* insertion were confirmed by sequencing (data not shown).

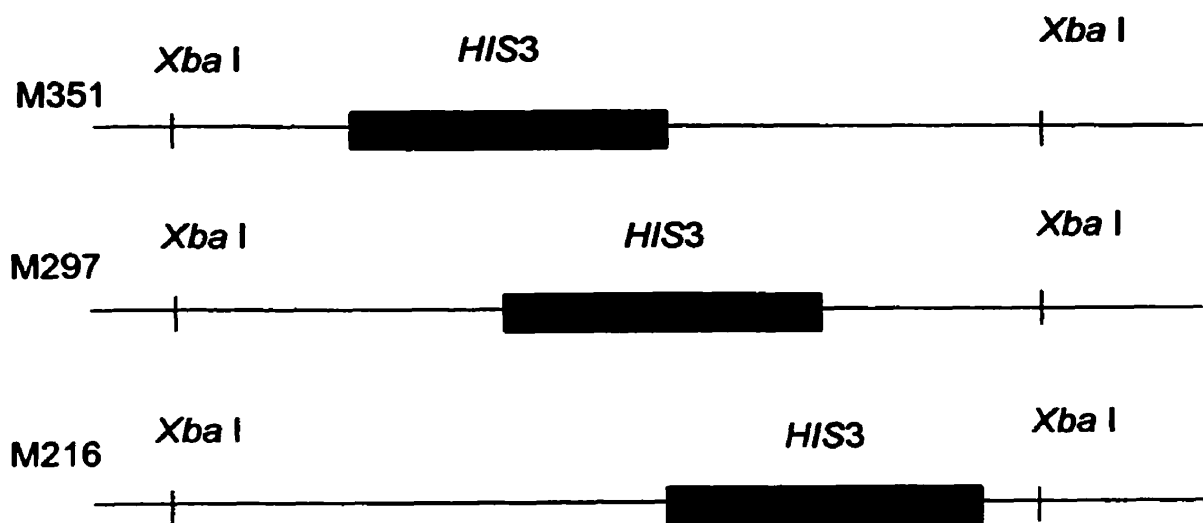
The generated mutant DNA was digested with *Xba*I, which released the F3::*HIS3* fragments as depicted in Figure 3.7; this allowed homologous recombination between mutant DNA and chromosomal *MIP1* gene when transformed into yeast strain YPH499. The transformation was carried out using the lithium acetate method described in (Gietz *et al.*, 1997) and positive clones were isolated on SC-HIS plates and subsequently plated on YPAD and YPG to ensure active growth under both fermentative and non-fermentative conditions. Mutants were checked for *HIS3* insertion by Southern blot hybridization using a *HIS3* probe and a *MIP1* probe for detection.

3.4. Development of the Southern blot probes

The *HIS3* probe was developed by *Bam*HI digestion of BS50 and isolation of the 1.7 kb *HIS3* fragment, which then was labeled using the DIG labeling system according to the manufacturer's protocols. All probes were dot blot tested for concentration according to DIG labeling system protocols.

A *MIP1* probe was created using the PCR primers developed for the production of the F3 amplicon. The resulting PCR fragments were isolated from a 1% agarose gel and labeled using the DIG labeling system.

Figure 3.7. Diagram of restriction digest to allow homologous recombination in yeast strain YPH499. *Xba*I was used to remove the mutated *MIP1* gene (thin line) with the *HIS3* marker gene insertion (filled box), from the plasmid DNA.



3.5. Southern blot hybridization

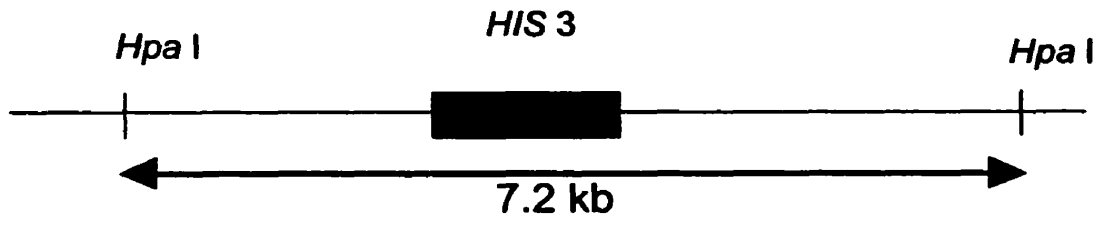
Genomic DNA of mutant cell lines was isolated using the methods described in Chapter 2 and the DNA was digested using the restriction enzyme *Hpa*I. This enzyme will cut genomic DNA in the *MIP1* gene, releasing the fragment containing the *HIS3* gene (Figure 3.8A/B). Following blotting to nylon membrane the genomic DNAs were probed with *HIS3* (Figure 3.8C) and *MIP1* (data not shown). The resulting Southern blot demonstrated that the *HIS3* marker was present within all four mutants (Figure 3.8C) in a fragment of the expected size. This fragment is not present in the wild-type DNA in which the *HIS3* gene has undergone a deletion of 1.1 kb (Figure 3.8B).

3.6. Growth characteristics of mutant cell lines

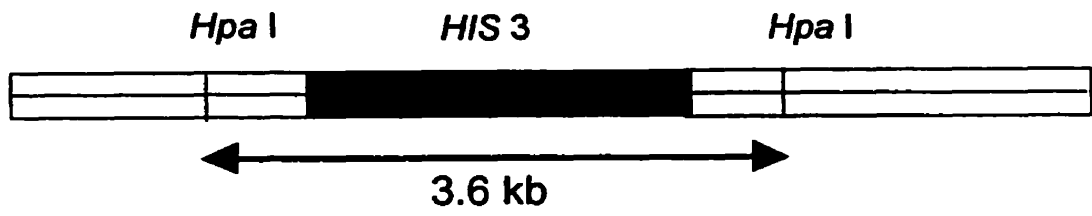
Normally *S. cerevisiae* grows with a doubling time of 90 min on glucose-based media at 30°C (Sherman, 1991). As a first step in characterizing the cells harbouring the truncated versions of Mip1p, the cells were grown at normal (30°C) and elevated (37°C) temperatures on glucose-containing media (YPAD). Mutant cells grew indistinguishably from wild-type (YPH499) on glucose-containing media (Figure 3.9). To determine maintenance of mitochondrial function under these conditions cells were removed at different time points and plated onto YPAD and glycerol-containing medium YPG. Loss of functional mtDNA during growth on YPAD would result in cells unable to grow on the non-fermentable carbon source glycerol. At 30°C, 80-100% of YPH499 and mutant cells maintained mitochondrial function as indicated by the ability to grow on YPG data not shown.

Figure 3.8. A. Diagram of *HIS3* region in YPH 499, with an internal deletion of 1042 bp. Thin and thick lines represent genomic DNA and *HIS3* gene respectively. Digestion with *HpaI* will result in a fragment of 7.2 kb that will be detected by the *HIS3* probe. B. Diagram of *MIP1* gene (open box) with inserted *HIS3* marker gene; digestion with *HpaI* will result in a fragment of 3.6 kb, which will be detected by the *HIS3* probe. C. Southern blot analysis of *HpaI*-digested genomic DNA from all four mutant cell lines (*Mip1p* Δ 351, *Mip1p* Δ 297, *Mip1p* Δ 216, and *Mip1p* Δ 176) and YPH 499, using a *HIS3* probe. Lanes 1-4, *Mip1p* Δ 351, *Mip1p* Δ 297, *Mip1p* Δ 216, and *Mip1p* Δ 176 respectively, demonstrate the presence of a band not seen in YPH 499 Lane 5. The additional band found in the mutant cell DNA is present from the insertion of the *HIS3* marker gene.

A



B



C

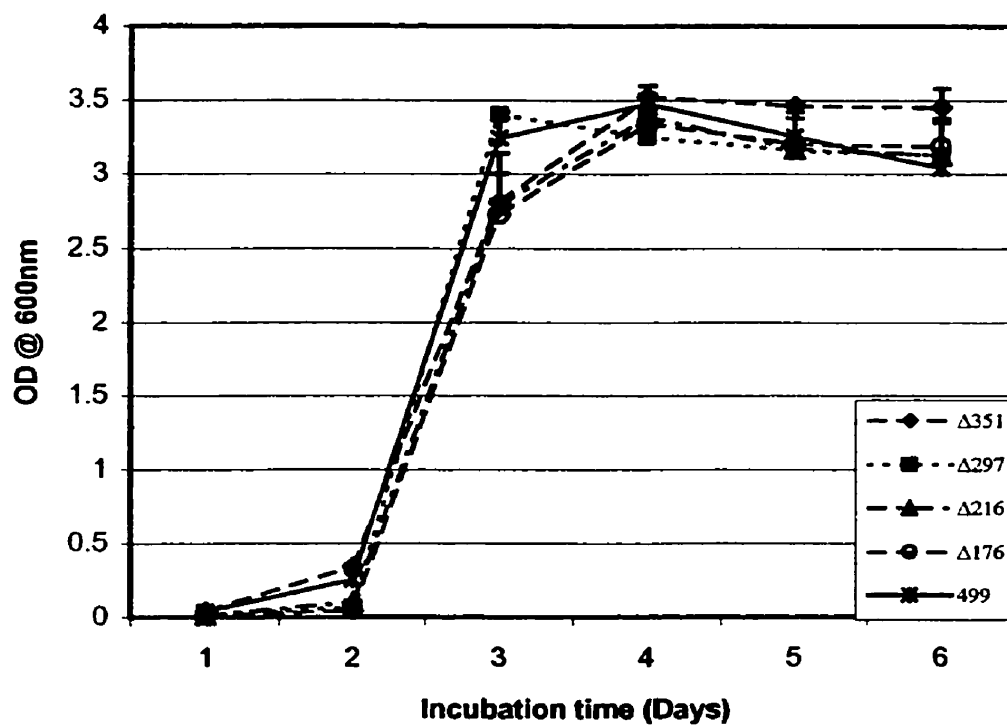
1 2 3 4 5



7.2 kb

3.6 kb

Figure 3.9. Growth characteristic of mutant cell lines and YPH499, grown in 10 mL YPAD broth at 30°C over 6 days; OD₆₀₀ readings were taken every 24 hours. The average of four experiments are presented , along with standard deviations.



The wild-type, *Mip1* Δ 176 and *Mip1* Δ 216 strains were also able to maintain mitochondrial function during one day (Figure 3.10) or up to five days of batch culture growth at 37°C (Figure 3.11). However, at this elevated temperature, strains expressing *Mip1* Δ 297 and *Mip1* Δ 351 rapidly lost the ability to grow on YPG; by 4.5 hours almost all *Mip1* Δ 351 cells and 80% of *Mip1* Δ 297 cells were unable to grow on non-fermentable carbon sources (Figure 3.10). Thus, at least 62 amino acid residues past the third polymerase domain in Mip1p are necessary for maintenance of mitochondrial function at 37°C.

Loss of mitochondrial function in *Mip1* Δ 351 and *Mip1* Δ 297 cells could be due either to loss of mtDNA entirely, or to mutation in mitochondrial genes essential for respiration and/or expression of respiratory complex proteins. To distinguish between these two possibilities, cells were stained with a DNA-specific stain DAPI after growth for varying lengths of time in YPAD (Figure 3.12/3.13). All cell types grown at 30°C maintained mtDNA staining, as expected from their ability to grow on non-fermentable carbon sources (Figure 3.10). However, cells expressing Mip1p Δ 351 and Mip1p Δ 297 lost mtDNA staining rapidly after being transferred to 37°C, while 80-100% of wild-type, *Mip1* Δ 216, and *Mip1* Δ 176 cells maintained cytoplasmic DAPI staining for at least five days. Thus, complete loss of mtDNA, rather than the accumulation of single mutations is responsible for the loss of respiratory ability in *Mip1* Δ 351 and *Mip1* Δ 297 cells.

3.7. Radioactive assay to determine polymerase activity

In order to confirm that the lack of mtDNA polymerase activity led to the loss of mtDNA from *Mip1* Δ 351 and *Mip1* Δ 297 cells at 37°C, we measured the rate of

Figure 3.10. Maintenance of respiratory competence during growth at 37°C. Wild-type and mutant cell lines were grown in YPAD broth for 8 hours at 30°C. Cell lines were diluted to 0.1 OD₆₀₀ in 10 ml YPAD and incubated at 37°C. Samples of the cell lines were removed every 90 min over 6 hours. Appropriate dilutions of cells were plated on YPG, YPAD, and SC-HIS. Data from plates that were grown for 2 days (YPAD) and 5 days (YPG) at 37°C were tabulated. The percent of respiratory competent cells was calculated as: [(Number of cells on YPG)/(Number of cells on YPAD)]x100. Each experiment was repeated four times; the average percentage of respiratory competent cells is plotted, along with standard deviations of the percentages.

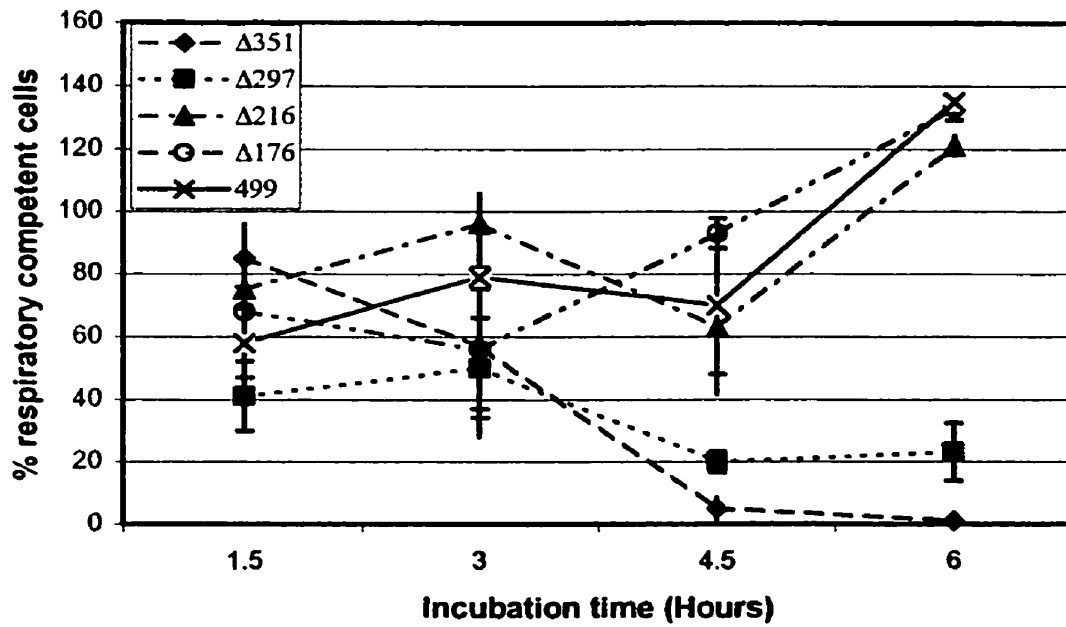


Figure 3.11. Maintenance of respiratory competence during growth at 37°C. Wild-type and mutant cell lines were grown in YPAD broth for 8 hours at 30°C. Cell lines were diluted to 0.1 OD₆₀₀ in 10 ml YPAD and incubated at 37°C. Samples of the cell lines were removed every 24 hours over 5 days. Appropriate dilutions of cells were plated on YPG, YPAD, and SC-HIS. Data from plates that were grown for 2 days (YPAD) and 5 days (YPG) at 37°C were tabulated. The percent of respiratory competent cells was calculated as: [(Number of cells on YPG)/(Number of cells on YPAD)]x100. Each experiment was repeated four times; the average percentage of respiratory competent cells is plotted, along with standard deviations of the percentages.

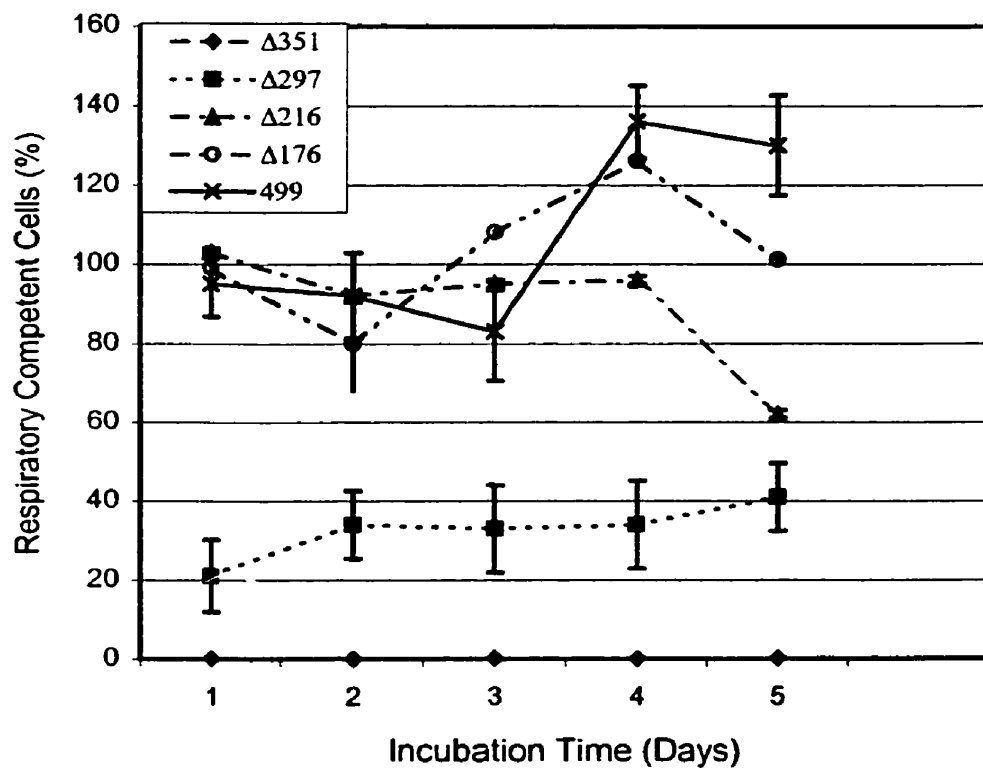


Figure 3.12. Mitochondrial DNA maintenance at 30°C. Wild-type and mutant cell lines were tested for the presence of mtDNA using 4,6 diamidino-2-phenylindole as described in Chapter 2. Samples of growing cells for mtDNA staining were taken at 0 hours, 6 hours, 24 hours, and 120 hours after dilution of 12-hour culture into YPAD. At each time point 100 cells of each type were visually assessed for the presence of mtDNA staining.

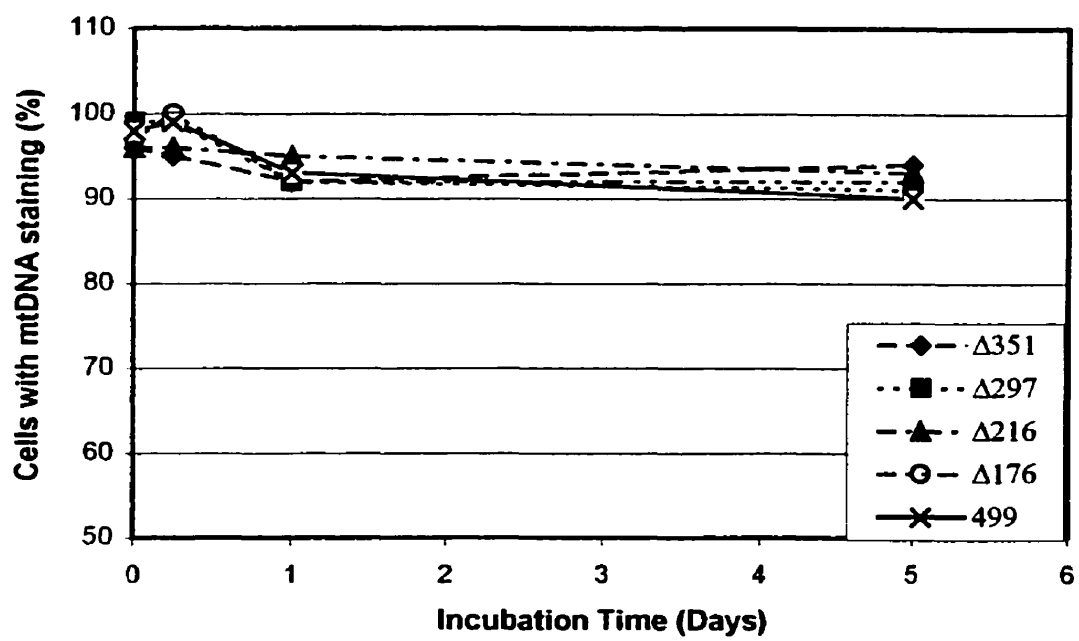
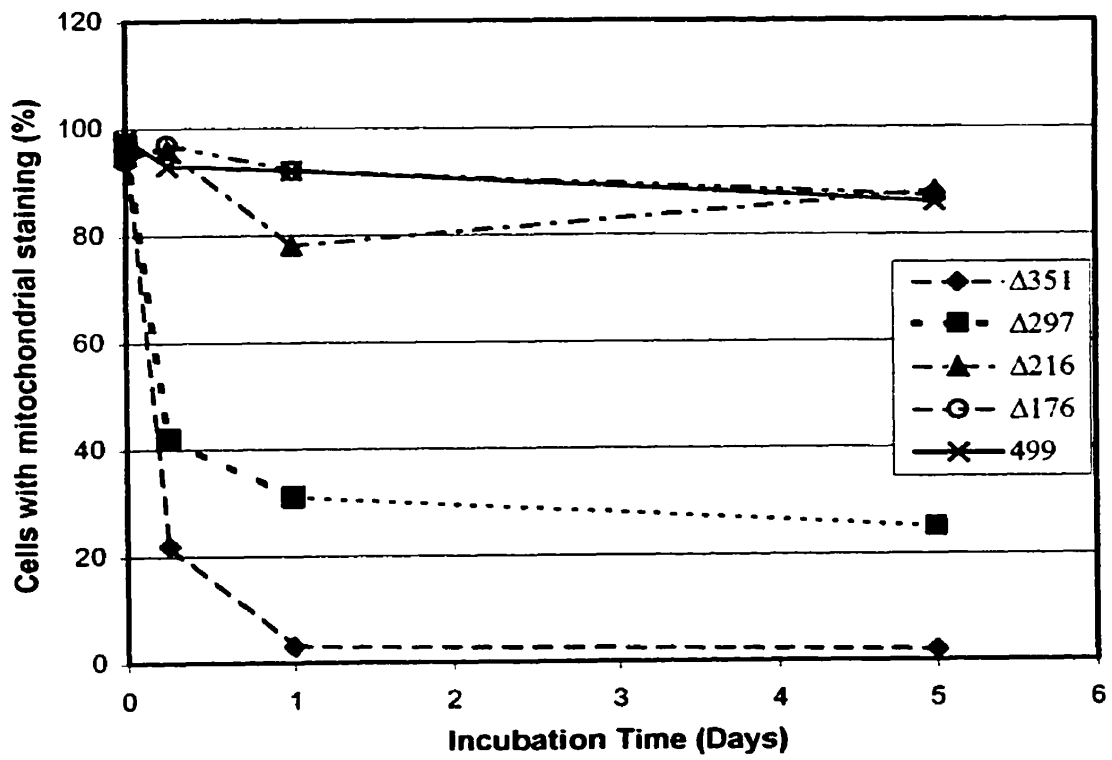


Figure 3.13. Mitochondrial DNA maintenance at 37°C. This experiment was performed as described for Figure 3.12 with the exception that the growth temperature was 37°C.



DNA synthesis in isolated mitochondria using radioactively-labeled dTTP.

Mitochondria were prepared from wild-type and mutant cells grown at 30°C and mtDNA polymerase activity was analyzed *in organello* to determine the replicative ability of the truncated versions of Mip1p.

When mtDNA was assayed at 30°C, no appreciable difference in radioactive incorporation was observed among the wild-type and mutant organelles (Figure 3.14). These observations are in agreement with the growth experiments, and together with the DAPI-staining results (Figure 3.12), indicate that all of the types of mitochondria contain approximately the same level of template DNA and polymerase.

To determine the effect of increased temperature on polymerase activity, the assays were repeated at 37°C. Wild-type, *MIP1Δ176*, and *MIP1Δ216* mitochondria incorporated radioactive nucleotides at levels slightly lower than those observed at 30°C (Figure 3.14). In striking contrast, *MIP1Δ351* and *MIP1Δ297* mitochondria demonstrated a large decrease in polymerase activity at 37°C (Figure 3.15). Incorporation by *MIP1Δ351* and *MIP1Δ297* mitochondria was less than 5% and less than 15%, respectively, of that by wild-type and *MIP1Δ176* mitochondria. Therefore, the loss of mtDNA from *MIP1Δ351* and *MIP1Δ297* cells is due to the lack of polymerase activity at this temperature.

Mitochondria from *MIP1Δ216* demonstrated a reproducible lag in incorporation, but the incorporation rate was similar to wild-type after 10 min of incubation (Figure. 3.15). The reason for this lag is unknown, but could be due to slow protein refolding or stabilization of interactions with other components of replication machinery after heat shock at 37°C.

Figure 3.14. *In organello* DNA synthesis by mutant and wild-type mitochondria. Mitochondria were isolated from cell lines grown at 30°C and incorporation of radioactive nucleotides was measured as described in Chapter 2 at 30°C. Each experiment was performed two to four times and average values and standard deviations for count per minute (cpm) of acid insoluble products are presented.

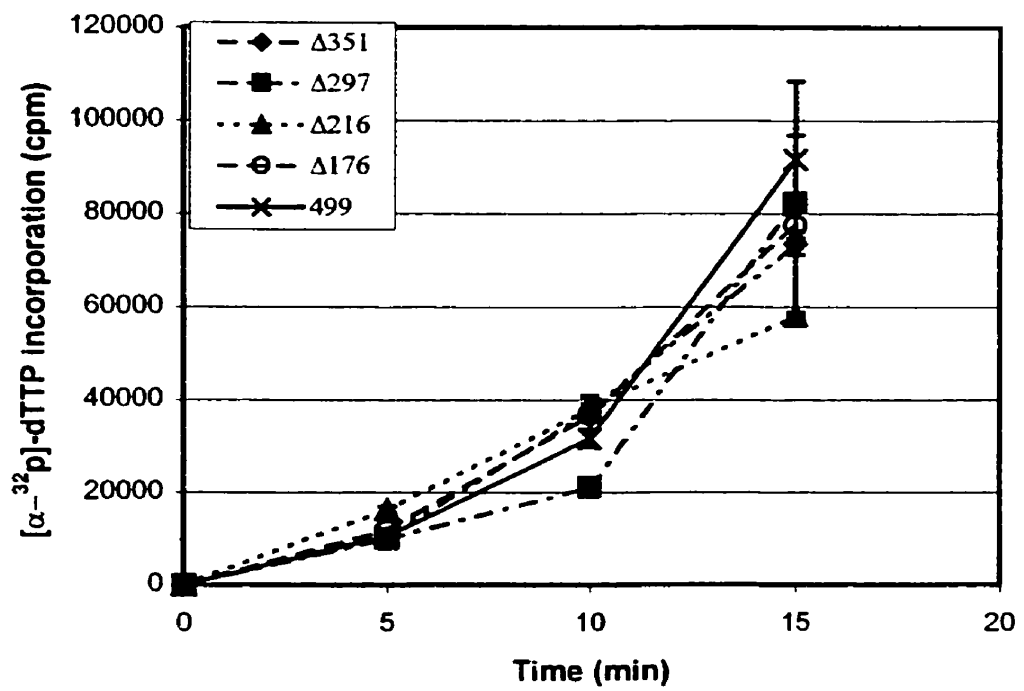
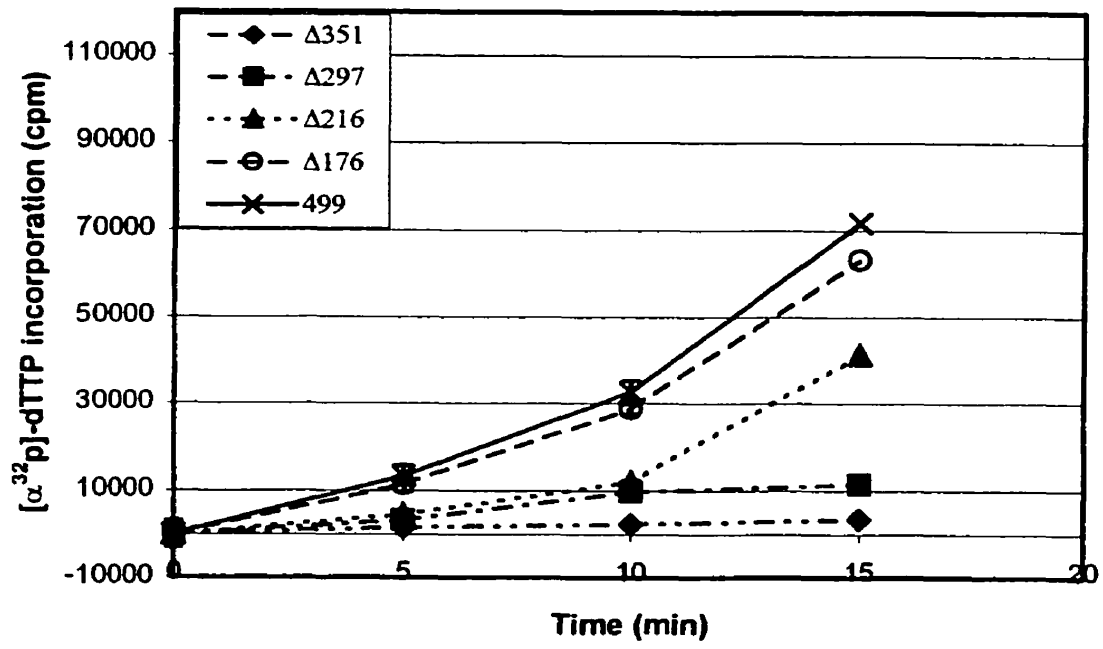


Figure 3.15. *In organello* DNA synthesis by mutant and wild-type mitochondria. Mitochondria were isolated from cell lines grown at 30°C and incorporation of radioactive nucleotides was measured as described in Chapter 2 at 37°C for the indicated times. Each experiment was performed four times and average values and standard deviations for count per minute (cpm) of acid insoluble products are presented.



3.9. Mip1p detection using Mip1p Antibody

We attempted to produce an antibody to Mip1p as described in Chapter 2. The lack of polymerase activity at 37°C could be due to the destabilization of the polymerase, or to the degradation of the enzyme. To distinguish between these two possibilities, we attempted to produce an antibody to Mip1p. Cloning of a 0.9 kb fragment from the Mip1 gene into the expression vector pQE10 was carried out according to the protocols in chapter 2. The purified protein was separated on a 7% SDS-PAGE gel (Figure 3.16) for visualization of a single protein product before being sent for antibody production. The antibody was first tested against purified HIS₆ MIP and whole bacterial isolated protein (Figure 3.17). The antibody was used to detect the Mip1p in whole mitochondrial extracts unfortunately little success was seen in the antibody binding to the Mip1p during western blot analysis. These results led us to the conclusion that the antibody may not specifically bind to Mip1p, this exhausted our binding assay attempts.

3.8 Discussion

Taken together, the results presented herein demonstrate that the carboxyl-terminal extension (CTE) of Mip1p is not essential for function of the polymerase at 30°C. This indicates that the amino acid residues in this portion of the enzyme do not make critical contacts with DNA, nucleotides or metal ions, nor do they make an essential structural contribution to the catalytic site of the enzyme. However, the segment of the CTE located nearest the putative catalytic domain of the protein appears to be required for function of the enzyme at high temperature. In particular, 62 residues past the third polymerase motif (residues 889-895) are required for

function at 37°C. The function of this segment of the protein is unclear. The required region includes residues 893-957, which are highly conserved among mitochondrial DNA polymerases, but do not share primary sequence similarity with the corresponding region in the bacterial and phage enzymes, which terminate about 60 residues after the third polymerase (P3) domain. In the Klenow fragment of *E. coli* DNA polymerase I (Ollis *et al.*, 1985) and in the T7 DNA polymerase (Doublet *et al.*, 1998), the segment to the C-terminal side of the P3 motif folds into a long α -helix, R, and β -strand 14. Neither of these structures directly contacts substrates or metal cofactors. A long α -helix is predicted for the corresponding region in the mitochondrial enzymes (residues 910 to 924 in Mip1p), but its location in the three-dimensional structure is unknown. Nonetheless, the presence of this putative α -helix alone is not sufficient for function at 37°C. It is possible that other sequences downstream of this helix are needed for correct folding of this part of the polymerase. Alternatively, this region of the enzyme may contribute to contacts with other proteins of the mtDNA replication machinery. Such proteins have not been identified for *Saccharomyces*, but it is possible that the enzyme utilizes protein factors that are critical, for example, for replication at high temperature. The overall stability of these interactions with Mip1p Δ 297 and Mip1p Δ 351 polymerases may be sufficiently weakened at 37°C to prevent mtDNA replication. Further insight into these possibilities requires greater understanding of the mitochondrial DNA replication machinery in fungi.

3.10 Future work

Possibilities of further work include, Circular dichroism studies of each mutant at permissive and non-permissive temperature. This would help in the determination of any structural differences in the mutant proteins at variable temperatures. Mutants could be produced which harbor mutations in the 62 residues past the third polymerases motif to determine the exact amino acid cut off for functional polymerase activity at 37°C. Also obtaining a 3-dimensional structure of Mip1p by X-ray crystallography would answer many questions about Mip1p bind to DNA. Using other temperatures that are not permissive to yeast could be used to determine if this temperature sensitivity seen in Mip1Δ351 and Mip1Δ297 is unique at 37°C.

Figure 3.16. Coomassie Blue stained SDS-PAGE of HIS₆Mip protein. Lane 1, Bacterial whole protein extract; lane 2, purified HIS₆Mip protein; lane 3, Low Molecular Weight Marker (Sigma). Each well was loaded with 2% of the total protein extracted.

1

2

3



66 kDa

45 kDa

36 kDa

29 kDa

Figure 3.17. Western blot of whole bacterial protein and purified HIS₆Mip protein extract. Each lane of the 12.5% SDS-PAGE gel was loaded with 2% of the total extracted protein from 1 liter of culture. After blotting to nitrocellulose, HIS₆Mip molecules were detected with an antibody against the N-terminus of Mip1p. The protein was detected at 35 kDa in both whole bacterial extract Lane, 3 and 4, and the purified HIS₆Mip extract lane, 1 and 2. The other band seen in the blot could be a break down product of the Mip1p.



35 kDa

APPENDIX

4.1. Autophagy project

4.1.1. Introduction

While completing a growth curve of YPH499 wild-type and mitochondrial mutant cell lines, we observed a contaminant that was present within enlarged vacuoles of all cell lines. This observation was clearly an unprecipitated event by the induced *MIP1* mutations, as the containment was present in the wild-type strain as well. New glycerol stocks of previous cell line isolation were grown in YPAD along with the glycerol stocks used in the above growth curve. Cells from the new glycerol stocks showed enlarged vacuoles in death phase, whereas those from the glycerol stocks used in the initial experiment showed enlarged vacuoles with spherical moving particles within the vacuoles in growth, stationary, and death phase. These particles will be referred to as spherical bodies throughout the following discussion.

These interesting results led to a literature review of possible answers explaining this interesting observation. This search led us to a process found in most eukaryotic organisms known as autophagy. Autophagy was first identified as the transport of cytoplasmic material to the vacuoles in response to nutrient deprivation, in which cells degrade large amounts of intracellular proteins for survival (Takeshige *et al.*, 1992). This type of lysosomal protein degradation is preformed by autophago-lysosomes that are formed by fusion of autophagosomes and vesicles containing lysosomal proteases or lysosomal membrane proteins. By

these means a cell can degrade unwanted or inactive proteins to recycle cellular components and increase nutrient supply during starvation.

Ohsumi's group of Tokyo Japan developed proteinase deficient mutants that would lack the ability to remove unwanted protein products (Takeshige *et al.*, 1992). It was shown that the enhancement of autophagic bodies was induced by the lack of proteinase A, proteinase B, and carboxypeptidase Y when cell were grown in nutrient deficient media (Takeshige *et al.*, 1992). It was demonstrated that cellular components including mitochondria, ribosomal subunits, and dysfunctional/functional proteins are sequestered to the vacuolar space under nutrient deficient phases of growth. Cell lines lacking proteinase A or proteinase B accumulated autophagic bodies within 2-3 hours after being grown in nutrient deficient broth. Conversely, wild-type cells showed a lack of autophagic accumulation within their vacuoles under starvation conditions for up to seven days (Takeshige *et al.*, 1992). Using proteinase deficient cell lines, Ohsumi's group was able to define the autophagic pathway present in *S. cerevisiae* (Tsukada and Ohsumi, 1993). Although these pathways are interesting, they are not critical in defining the cause of the spherical bodies seen in our experiment; what is more pertinent to our needs is the morphological study of autophagic bodies.

4.1.2. Experimental plan

A few concerns about the validity of what was seen in our experiments and what is known to be present in autophagy are compelling. In our experiments spherical bodies in enlarged vacuoles were seen after 12 hours of growth in nutrient broth, at this point cells would be in stationary phase. These spherical

bodies also showed tumble and run movement within the vacuoles and out side in the medium, rather than Brownian movement seen in normal autophagic body production. These two results lead us to the conclusion that these spherical bodies in our cell lines were not autophagosomes and were in-fact an artifact of unknown origin.

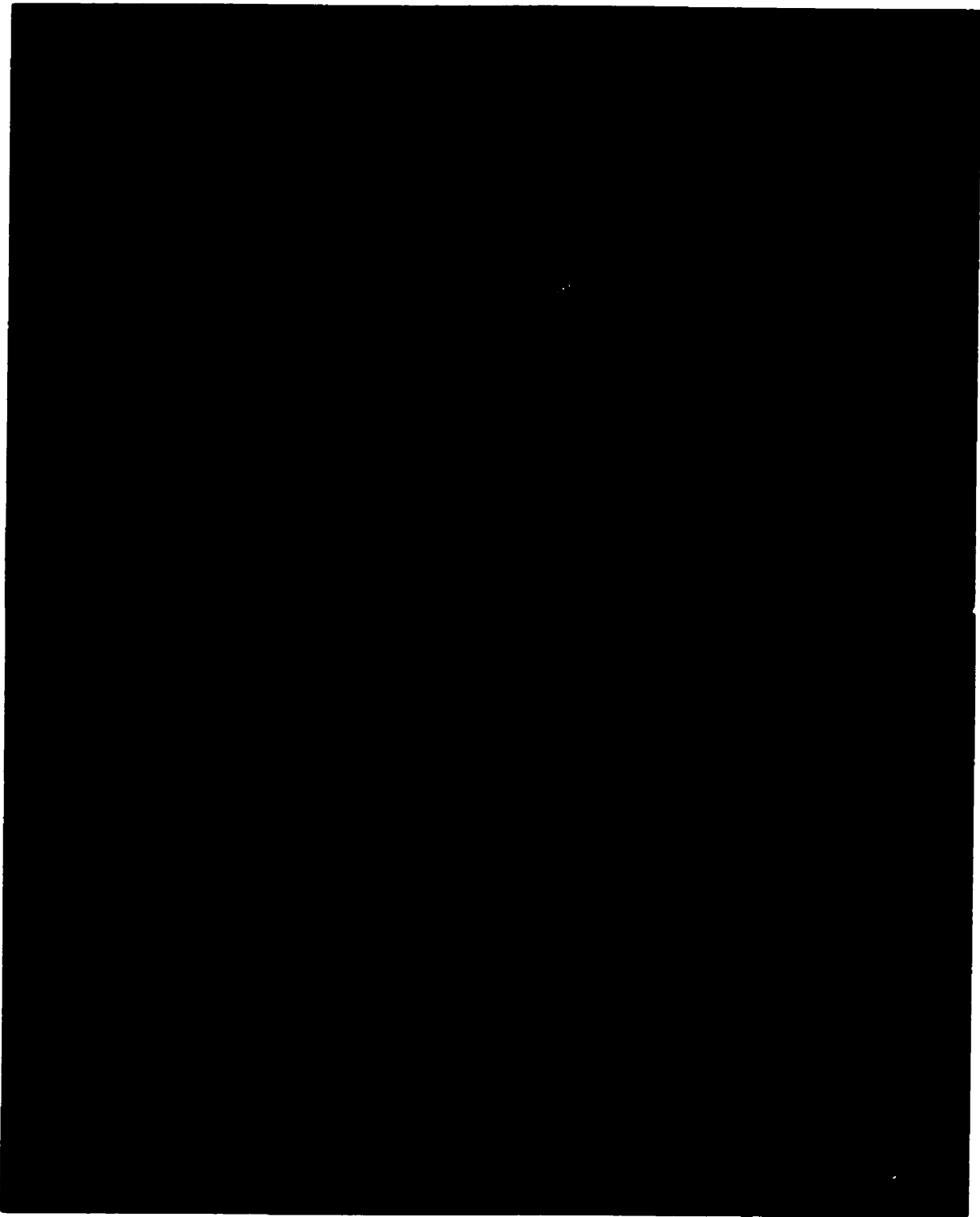
Once the determination was made that we were not looking at autophagy a plan was developed to define what these spherical bodies could be. Our first experiment was to ensure that these spherical bodies had no resemblance to autophagic bodies, using phenylmethylsulfonyl (PMSF) to inhibit proteinase A and proteinase B and thereby force the induction of autophagsomes (Takeshige *et al.*, 1992). PMSF was used on a new wild-type strain of YPH499 (new glycerol stock), one that showed no spherical body production after 12 hours of growth in nutrient deprived media. Comparing the spherical body containing cell culture with the PMSF-induced autophagic cell culture a marked difference was seen. The PMSF cell culture demonstrated characteristic autophagic production as described above and in Takeshige *et al.*, (1992), with an absence of autophagic body production outside of the yeast cells. The spherical body cell cultures showed run and tumble movement of these bodies with the presence of numerous spherical bodies outside of the yeast cell. The spherical bodies outside of the yeast cells demonstrated a run and tumble movement, which is not characteristic of autophagic bodies.

To further strengthen the thought that the spherical bodies are not autophagic bodies and are in-fact bacteria, an attempt to isolate the spherical bodies was

carried out. We first attempted to grow the yeast cultures with spherical bodies using increasing dilutions on LB agar; this method was used to try to isolate individual colonies of both yeast and spherical bodies. As above, isolation attempts were carried out using potato extract agar, YPAD agar, and T-soy agar. All pure culture experiments were unsuccessful at isolating spherical bodies, although many yeast colonies with uncharacteristic colony morphology were seen! Since the spherical bodies were difficult to isolate from the yeast cells we carried out new pure culture experiments by first treating the yeast cells with Lyticase (Sigma) at 2 μ g/ml concentrations, then plated them on YPAD, LB, and T-soy agar plates. Treatment with lyticase will disrupt the cell wall of the yeast cells and should allow the spherical bodies to grow unhindered by the yeast cells. Unfortunately, the yeast cells could repair the induced cell wall damage and grow normally during the incubation period of the experiment. During the above isolation attempts photographs were taken of the yeast cells with spherical bodies (Figure 4.1). These photographs represent yeast cells with spherical bodies within enlarged vacuoles and spherical bodies outside the yeast cells in the medium.

Other methods used to separate the spherical bodies from yeast cells included treatment with antibiotics. This type of treatment takes into account the differences between eukaryotic and prokaryotic cell walls. Ampicillin at 50 mg/ml was used to disrupt the 'growth' if any of these spherical bodies. After treatment with ampicillin, spherical bodies were still seen inside the yeast cells vacuoles and outside the cells. This would indicate that the containment (spherical bodies) are

Figure 4.1. Photographs of cells with enlarged vacuoles, these enlarged vacuoles carrier spherical particles, cell were photographed using 100X oil emersion on a Zeiss microscope. V indicates vacuoles and S illustrates spherical bodies.



unaffected by ampicillin or they are not actively growing. Rifampicin, which interrupts DNA or RNA metabolism within bacteria by binding to the DNA-directed RNA polymerase, was also used at 50mg/ml concentrations as antibiotic to remove spherical bodies. Interestingly spherical bodies outside the cells were removed. But, the spherical bodies within the enlarged vacuoles were still present which, could be attributed to the lack of antibiotic transfer into the cell. These results show that the spherical bodies are removed from the supernatant using antibiotics. This indicates the possibility that the spherical bodies are in-fact living bacterial-type organisms.

The above results promoted us to do growth studies of a new yeast cell line with no possible prior exposure to spherical bodies, and the cell lines that show spherical body contamination. The cultures were grown in YPAD broth, every 24 hours an optical density was measured and used to calculate the cell density. This data was used to inoculate new YPAD medium 10 ml at a cell density of 0.1 OD. Samples of the culture at the end of each growth day and at 6 hours after inoculation were removed for microscopic observation. The growth of the cultures were found to be similar in OD number, smell and color. Microscopic observation showed two main differences: the pure yeast culture showed very few autophagic bodies with no autophagic bodies outside of the yeast cells. The autophagic bodies were ~ 1/1000 to 1/10 the size of the yeast cells. The culture with spherical bodies had these bodies outside the cells which were ~ 1/1000 the size of yeast cells. There were also spherical bodies within the vacuoles of the yeast cells which were ~ 1/1000 the size of yeast cells. This experiment further concludes that there are

many differences between the new yeast cultures and the suspected contaminated culture.

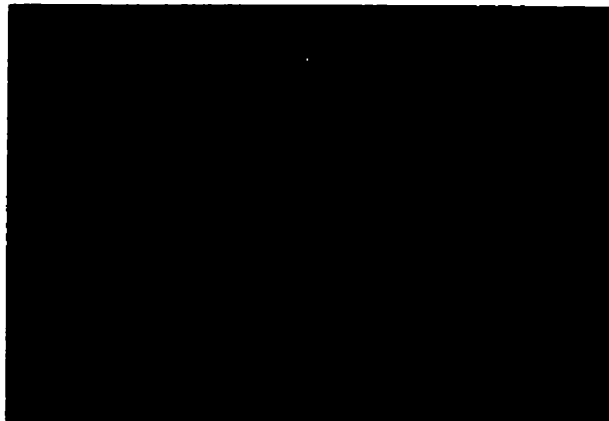
Other attempts to prove Koch's postulates in regards to these spherical bodies were taken. These included vacuolar isolation in which lysis of the vacuole could be carried out and pure culture isolation using differential centrifugation could be used to study the spherical bodies. Unfortunately, the amount of vacuoles that was isolated was insufficient to allow isolation spherical bodies at a concentrations that would allow other experimentation.

The above experiments led us to more morphological studies of these spherical bodies. The first experiment used was DAPI staining using spherical body infected mtDNA deficient strains of *S. cerevisiae* and wild-type *S. cerevisiae*. Samples were grown for 6 hours in 10 ml YPAD, 2 ml was spun down and resuspended in 50 ml of ddH₂O. DAPI was added to a final concentration of 0.1-0.2 µg/µl and viewed using a Zeiss Epi-fluorescent microscopy. As depicted in Figure 4.3 the mitochondrial deficient strains showed yellow circular particles in about 10% of the cells, when looked at under light microscopy conditions these cells had enlarged vacuoles with moving particles within them. In contrast the wild-type strains had no yellow particles present at all, the only visible structures other than DAPI stained nucleus was mitochondrial stained DNA Figure 4.2. These results clearly indicate that these spherical bodies are something unique!

Using electron microscopy was the next logical step; if internal structures could be identified which are bacterial then we could conclude that these spherical bodies are in-fact bacteria. Cells of both wild-type YPH499 non-contaminated and

Figure 4.2. A. DAPI stained mtDNA free yeast cell with spherical bodies within the vacuoles. The spherical bodies stain a bright yellow this yellow staining is only present in yeast cells with spherical bodies. B. DAPI stained yeast cells, these cells mtDNA and nuclear DNA stain blue, which is characteristic of DAPI staining.

A



B



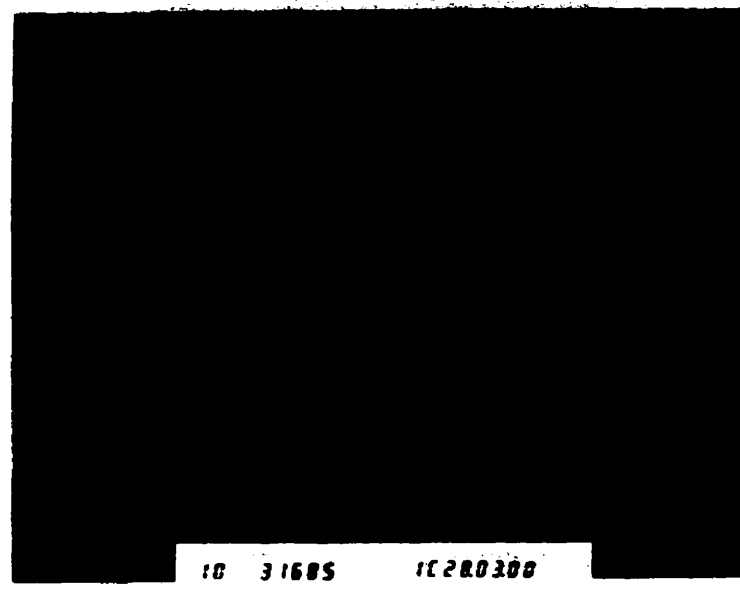
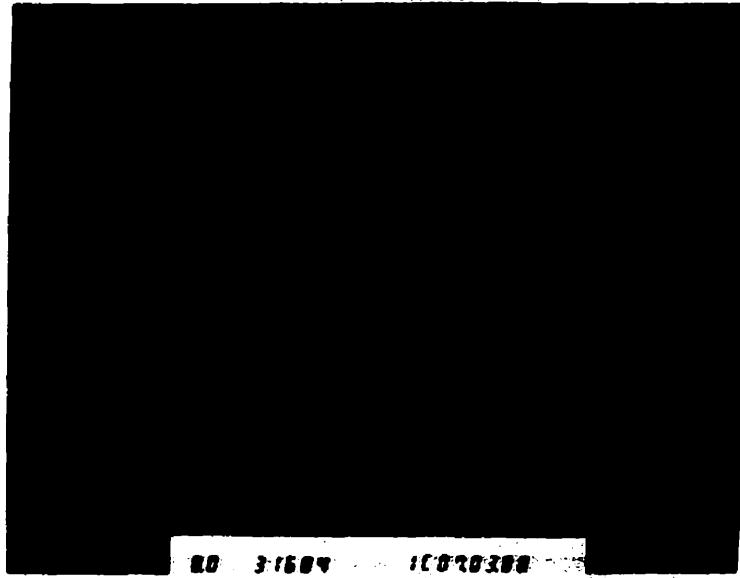
contaminated were used for the electron microscopy experiment. Cell cultures were grown to a final concentration of 5×10^6 cells/ml in YPAD. Cells were pelleted and fixed using 4% glutaraldehyde and 4% paraformaldehyde. The cell wall was removed using Zymolyase at a concentration of 0.5 mg/ml in 0.1 M phosphate-citrate buffer, postfixation and En bloc staining was carried using potassium permanganate and osmium ferricyanide receptively. Dehydration of the sample was carried out using Spurr's formula and the samples were thin section cut and placed on grids by Lynn Burton (Dept. of Botany). As figure 4.3 demonstrated the method used did not define the spherical particles, although they are present in the electron microscopy picture internal structures are difficult to see!

4.1.3. Future work

This project unfortunately was stopped to further the research in the main body of this thesis, but other experiments that could be carried out include 16S rRNA sampling of the contaminated samples. Koch's postulates could be proven by infecting non-infected samples and testing transfer of the contaminate using DAPI staining; this could illustrate transfer of the unique yellow particles when stained with DAPI.

Figure 4.3. Electron micrographs of YPH499 cells infected spherical bodies.

Structural distinction between spherical bodies and YPH499 internal structure are poor due the staining method used.



References

- Biswas, T.K., Sengupta, P., Green, R., Hakim, P., Biswas, B., Sen, S. (1989). Properties of mitochondrial DNA polymerase in mitochondrial DNA synthesis in yeast. *Acta Biochim. Pol.* 42, 317-324.
- Bolden, A., Noy, G.P., Weissbach, A. (1976). DNA polymerase of mitochondria is a gamma-polymerase. *J. Biol. Chem.* 252, 3351-3356.
- Braithwaite, D., Ito, J. (1993). Compilation, alignment, and phylogenetic relationships of DNA polymerases. *Nucl. Acids Res.* 21, 787-802.
- Carrodeguas, J.A., Kobayashi, R., Lim, S.E., Copeland, W.C., Bogenhagen, D.F. (1999). The accessory subunit of *Xenopus laevis* mitochondrial DNA polymerase γ increases processivity of the catalytic subunit of human DNA polymerase γ and is related to class II aminoacyl-tRNA synthetases. *Mol. Cell Biol.* 19, 4039-4046.
- Daum, G., Bohni, P.C., Schatz, G. (1982). Import of proteins into mitochondria. *J. Biol. Chem.* 257, 13028-13033.
- Doublet, S., Tabor, S., Long, A.M., Richardson, C.C., Ellenberger, T. (1998). Crystal structure of a bacteriophage T7 DNA replication complex at 2.2 Å resolution. *Nature* 391, 251-258.
- Foury, F. (1982). Repair of mitochondrial DNA in *Saccharomyces cerevisiae*. *J. Biol. Chem.* 257, 781-787.

- Foury,F. (1989). Cloning and sequencing of the nuclear gene MIP1 encoding the catalytic subunit of the yeast mitochondrial DNA polymerase. *J.Biol.Chem.* 264, 20552-20560.
- Foury,F., Vanderstraeten,S. (1992). Yeast mitochondrial DNA mutators with deficient proofreading and exonucleolytic activity. *EMBOJ* 11, 2717-2726.
- Genga,A., Bianchi,L., Foury,F. (1989). A nuclear mutant of *Saccharomyces cerevisiae* deficient in mitochondrial DNA replication and polymerase activity. *J.Biol.Chem.* 261, 9328-9332.
- Gietz,R.D., Triggs-Raine,B., Robbins,A., Graham,K.C., Woods,R.A. (1997). Identification of proteins that interact with a protein of interest: Application of the yeast two-hybrid system. *Mol.Cell Biol.* 17:67-79
- Hanahan,D. (1983). Studies on transformation of *Escherichia coli* with plasmids. *J.Mol.Biol.* 166-557.
- Ito,J., Braithwaite,D. (1990). Yeast mitochondrial DNA polymerase is related to the family A DNA polymerase. *Nucl.Acids Res.* 18, 6716-6716.
- Ito,J., Braithwaite,D. (1991). Compilation and alignment of DNA polymerase sequences. *Nucl.Acid Res* 19, 4045-4057.
- Johnson,A.A., Tsai,Y.C., Graves,S.W., Johnson,K.A. (2000). Human mitochondrial DNA polymerase holoenzyme: reconstitution and characterization. *Biochemistry* 39, 1702-1708.

- Kitto,G.B. (1969). Intra-and extramitochondrial malate dehydrogenases from chicken and tuna heart. *Meth.Enzymol 13*, 106-113.
- Kunkel,T.A., Roberts,F.D., Zakour,R.A. (1987). Rapid and efficient sit-specific mutagenesis without phenotypic selection. *Meth.Enzymol 154*, 367-382.
- Lecrenier,N., Van Der,B.P., Foury,F. (1997). Mitochondrial DNA polymerases from yeast to man: a new family of polymerases. *Gene 185*, 147-152.
- Ollis,D.L., Brick,P., Hamlin,R., Xuong,N.G., Steitz,T.A. (1985). Structure of large fragment of *Escherichia coli* DNA polymerase I complex with dTMP. *Nature 313*, 762-766.
- Pavco,P.A., Van Tuyle,G.C. (1985). Purification and general properties of the DNA-binding protein (P16) from rat liver mitochondria. *J.Cell.Biol 100*, 258-264.
- Ropp,P.A., Copeland,W.C. (1996). Cloning and characterization of the human mitochondrial DNA polymerase, DNA polymerase gamma. *Genomics 15*, 449-458.
- Sambrook,J., Fritsh,E.F., and Maniatis,T. (1989). "Molecular cloning. *A laboratory manual*". Cold Spring Harbor Laboratory.
- Sherman,F. (1991). *Meth.Enzymol 194*, 3-21.
- Sikorski,R.S., Hieter,P. (1989). A system of shuttle vectors and yeast host strains designed for efficient manipulation of DNA in *Saccharomyces cerevisiae*. *Genetics 122*, 19-27.

- Steger,H.F., Sollner,T., Kiebler,M., Dietmeier,K.A., Pfaller,R., Trulzsch,K.S., Tropschug,M., Neupert,W., Pfanner,N. (1990). Import of ADP/ATP carrier into mitochondria: two receptors act in parallel. *J. Cell Biol.* 111:2353-2363.
- Takehige,K., Baba,M., Tsuboi,S., Noda,T., Ohsumi,Y. (1992). Autophagy in yeast demonstrated with proteinase-deficient mutants and conditions for its induction. *J.Cell.Biol* 119, 301-311.
- Thompson,J.D., Higgins,D.G., Gibson,T.J. (1994). Clustal W; Improving the sensitivity of progressive mutiple sequence alignment through sequence weighting, position specific gap penalties an dweight matrix choice. *Nucl.Acid Res* 22, 4673-4680.
- Tsukada,M., Ohsumi,Y. (1993). Isolation and characterization of autophagy-defective mutants of *Saccharomyces cerevisiae*. *FEBS* 333, 169-174.
- Villarejo,M.R., Zabin,I. (1974). β -Galactosidase from termination and deletion mutant strains. *J.Bacteriol.* 120, 466-474.
- Weissbach,A., Baltimore,D., Bollum,F., Gallo,R., Korn,D. (1975). Nomenclature of eukaryotic DNA polymerase. *Science* 401-402.
- Yoneda,M., Bollum,F. (1965). Deoxynucleotide-polymerizing enzymes of calf thymus gland. *J.Biol.Chem.* 240, 3385-3391.